BERKELEY LAB

ERNEST ORLANDO LAWRENCE
BERKELEY NATIONAL LABORATORY

RECEIVED
MAY 12 1997
OSTI

Energy & Environment Division

Environmental Research Program

1995 Annual Report

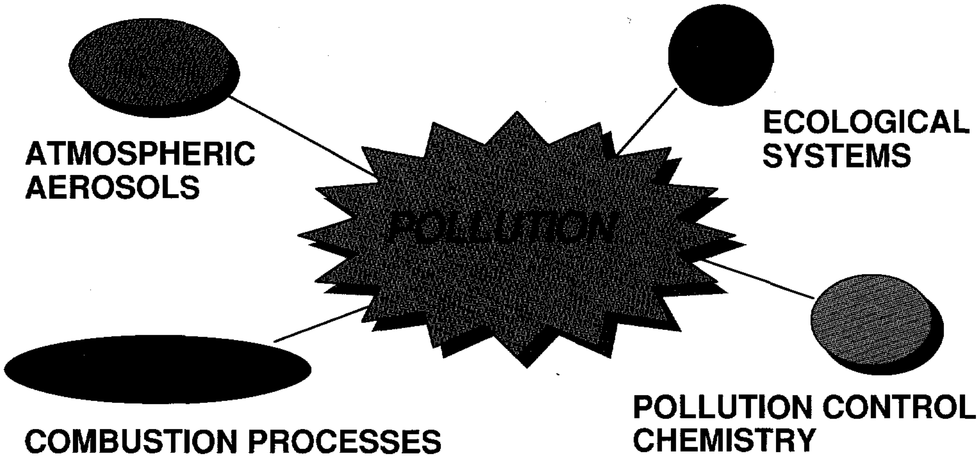

June 1996

MASTER

Cover: The Environmental Research Program performs research to enhance the understanding and mitigate the effects of pollutants on health, ecological systems, global and regional climate, and air quality.

Available to DOE and DOE Contractors from
Office of Scientific and Technical Information
P.O. Box 62, Oak Ridge, TN 37831
Prices available from (615) 576-8401

Available to the public from
National Technical Information Service
U.S. Department of Commerce
5285 Port Royal Road, Springfield, VA 22161

Prepared for the U.S. Department of Energy under Contract No. DE-AC03-76SF00098

Environmental Research Program
1995 Annual Report

Nancy J. Brown, Program Head

Energy & Environment Division
Ernest Orlando Lawrence Berkeley National Laboratory
University of California
Berkeley, California 94720
(510) 486-5001

Report No. LBL-38353

Contents

INTRODUCTION

Flue-Gas Chemistry

Combustion

Atmospheric Processes

Ecological Systems

SPONSORS

Introduction

The objective of the Environmental Research Program is to enhance the understanding of, and mitigate the effects of pollutants on health, ecological systems, global and regional climate, and air quality. The program is multidisciplinary and includes fundamental research and development in efficient and environmentally benign combustion, pollutant abatement and destruction, and novel methods of detection and analysis of criteria and noncriteria pollutants. This diverse group conducts investigations in combustion, atmospheric and marine processes, flue-gas chemistry, and ecological systems.

Combustion chemistry research emphasizes modeling at microscopic and macroscopic scales. At the microscopic scale, functional sensitivity analysis is used to explore the nature of the potential-to-dynamics relationships for reacting systems. Rate coefficients are estimated using quantum dynamics and path integral approaches. At the macroscopic level, combustion processes are modelled using chemical mechanisms at the appropriate level of detail dictated by the requirements of predicting particular aspects of combustion behavior. Parallel computing has facilitated the efforts to use detailed chemistry in models of turbulent reacting flow to predict minor species concentrations.

Investigations in turbulent combustion have resulted in development of a laboratory burner that produces very intense turbulent flames. It can be used for fundamental research of turbulence-flame interactions under the conditions encountered in most practical devices. It is also ideal for future work on ignition and extinction phenomena. With the award of a DOE Energy Research Laboratory Technology Transfer Cooperative Research and Development Agreement with Teledyne-Laars in Moorpark, California, a program is underway to commercialize the weak-swirl burner for use in small to medium water heaters. The focus is to develop a production prototype operating at 10 to 50 kW. Progress in the investigation of flame-gravity coupling includes completing a series of microgravity experiments on board a Learjet. The results help to identify the gravitational influences on flame propagation.

In the past year, the Chemical Treatment Processes Group has focused on controlling and converting atmospheric and aqueous pollutants. They have continued to develop techniques for converting NO, SO_2, and CO_2, which are pollutants from energy generation. The simultaneous removal of SO_2 and NO from flue gas by using an aqueous mixture of limestone and an iron compound has been successfully demonstrated on a bench-scale scrubber. In addition, a catalyst which is capable of converting SO_2 to elemental sulfur in the presence of moisture has been developed. A new, phosphorus-based process called POZONE has been developed and has been applied to help paper manufacturers bleach white paper without creating wastewater that contains hazardous chlorinated-organic compounds.

Research on the use of laser fragmentation for measuring toxic metal species has yielded new information on the formation of particles containing metal species. Measurements of the metals can be

(cont.)

Program Staff

Nancy J. Brown[*], *Program Head*

Lisa Alvarez-Cohen
Susan Anderson
Frank Asaro
Benoit Bedat[†]
Steven Buckley[†]
Johnny Chang
Shih-Ger Chang[*]
Jyh-Yuan Chen
Steve Chen
Robert Cheng
Craig Corrigan
Robert Dibble
Carlos Fernandez-Pello
Heather Freeman
Gale Garman[†]
Regine Goth-Goldstein
Robert Giauque
Gloria Gill
Iskander Gokalp[†]
Ralph Grief
Robert A. Harley
John Harte
Jennifer Hoffman
Jack Hollander[†]
Kenneth Hom
Gary Hubbard
Kewu Huang[†]
James Hunt
Mary Hunt
John Jelinski
David Jenkins
Yun Jin[†]
Jay Keasling
John Knezovich[†]
Cheong Ki Chan[†]
Thomas Kirchstetter[†]
Stevan Jovanovich
Hirotsugu Kobuchi
Michael Koszykowski[†]
Catherine Koshland
Guoping Li
David Littlejohn
Donald Lucas
Robert Macey
John Maguire
Rolf Mehlhorn
Katherine Moore
Tihomir Novakov[*]
Antoni Oppenheim
Lester Packer
Patrick Pagni
Joyce Penner[†]
Robert Risebrough
Carlos Rivera-Carpio
C. Fredrick Rogers[†]
Walter Sadinski[†]
Robert Sawyer
Richard Schmidt
David Sedlak
Ian Shepherd
Yao Shi[†]
Martyn Smith
Fred Stross[†]
Lawrence Talbot
Chang-Lin Tien
Hai Wang[†]
Shu-Mei Wang[†]
R. Brady Williamson
Andrew Wilson[‡]
Linda Wroth
Laurent Vuilleumier[†]
Qiquan Yu[†]
Derek Yegian

---

[*] Group Leader
[†] Participating Guest
[‡] Student Assistant

conducted both in the gas phase and condensed in aerosols in combustion environments. Methods are being developed to quantify these species.

Thermal destruction of chlorinated hydrocarbons are being studied, and these have revealed new information about the reaction pathways of benzene and chlorobenzene in the post-flame environment.

A new study of the emissions from heavy oil storage tanks has been initiated. Existing techniques of analysis are being extended to the higher temperatures found in storage tanks, and new methods are under evaluation for the quantification and speciation of organic vapors.

Research in our Atmospheric Aerosol Group is concerned with contributing to our understanding of the role of aerosol particles in climate forcing. Aerosol particles control the intensity of visible and UV radiation reaching Earth's surface. These particles affect Earth's climate by scattering and absorption of solar radiation and by influencing the number concentration of cloud droplets (and cloud albedo) through their ability to act as cloud condensation nuclei. Although most of the mass of anthropogenic aerosol is composed of sulfates, organic material, nitrates, and mineral dust, sulfate aerosol receives the most attention because of its relatively well-documented global distribution and its known optical and nucleation properties. There are significant uncertainties associated with predicting the aerosol effects on climate if the nonsulfate aerosols, particularly organic aerosols are not taken into account.

The significance of organic aerosols is suggested by the facts that concentrations of these species often exceed the concentrations of sulfates, that their optical properties are comparable to sulfate, and that organic aerosol material is largely water soluble and acting as efficient CCN. LBNL research is contributing to understanding the role of organic aerosols in radiative transfer and in cloud formation.

Program scientists have begun to quantify model uncertainty in air quality modeling. They have initiated the development of a gradient-based sensitivity approach, and are applying it to a smog chamber model.

Experiments and calculations of the Environmental Research Program confirmed that the use of polarization sensing techniques can reduce scattered light components and therefore improve visibility in the Marine Boundary Layer (MBL) Project. Our studies have shown that the optimum orientation of the polarizer and its efficacy in improving image contrast depends on both atmospheric conditions and the solar (illumination source)-viewer-target angle. Furthermore, as MBL aerosols are highly complex and variable, mixtures that have profound effects on visibility and radiance calculations, designing an agile polarization-sensing device to optimize strategies for improving visibility and image discrimination under various conditions would be especially prudent. Our calculations and experimental work indicate that Mie calculations can produce reliable inputs for calculating radiant transfer under most (except very dry air) atmospheric.

Programs in ecological systems are diverse, ranging from genetic ecotoxicology to studies of global climate change. Researchers in the Genetic Ecotoxicology Research Laboratory have investigated the relationship between genotoxic response and reproductive success in aquatic organisms. Specifically, they established this relationship for two animal models—sea urchins and nematodes. They developed an assay using sea urchins to evaluate effects of exposure to UV-B—the first animal model to evaluate the genotoxic effects of Antarctic ozone depletion. They have established that ambient levels of UV-A and UV-B have significant effects on sea urchin embryos in Antarctica, even after peak ozone depletion. LBNL ecotoxicology scientists have also performed an important role in establishing broad priorities for the field of ecotoxicology. The group has begun a successful collaboration with researchers from U.C. Davis in a remediation effort at Mare Island.

Program scientists seek biological solutions to environmental contamination problems. The studies comprise two aspects: (1) efforts to better understand toxicity mechanisms and (2) the development of schemes for the removal and recovery of environmental contaminants. They have observed that a major toxicity mechanism of tobacco smoke in blood is enzyme inhibition by cyanide. Studies with textile dyes have lead to the development of several biomass systems that remove selected organic molecules from water.

In a new program, research has been initated in wound healing. During the immune response to a bacterial infection, bacteria need to be killed or rendered harmless. White blood cells (leukocytes) both in the circulating and in the peripheral tissues have enzyme systems that can specifically take up and kill bacteria. Our research effort has resulted in defining new ways to enhance the activity of NADPH-oxidase, which is a major enzyme involved in leukocyte killing. Using added exogenous antioxidants we have been able to enhance the rate and extent of this important immunological enzyme. These studies are a prelude to further studies to determine the role of antioxidants in leukocytes and their relationship to immunity.

Program biologists are developing new approaches to evaluate the health risk of environmental pollutants to humans by using human cell culture systems as surrogates to animal testing. They have established an assay to evaluate the presence of polycyclic aromatic hydrocarbons in complex mixtures of pollutants.

Program scientists have worked with other investigators within the Energy and Environment, Earth Sciences, Life Sciences, and Information and Computing Sciences Division on the SELECT project. The goal of the SELECT project is to design and develop a distributed, object-oriented computer architecture to integrate, analyze, and present environmental information to help managers select cost-effective environmental remediation that maximizes health-risk reduction while minimizing costs. A salient feature of the architecture is incorporation of state-of-the-art scientific advances in site characterization, subsurface and atmospheric transport processes, exposure pathway analyses, and health-hazard assessment, as well as financial analyses of environmental remediation. Researchers in our program have developed an air transport model that is useful for exposure calculations. Comparison of estimated cancer risks from background exposures (*e.g.*, from indoor sources or natural chemicals in the diet) with potential exposures from the contaminant site has been incorporated.

Flue-Gas Chemistry

NO Absorption Studies with $Fe^{2+}(DMPS)_2$ Solutions

Y. Shi, H. Wang, D. Littlejohn, and S-G. Chang

We recently developed a new ferrous thiochelate additive, $Fe^{2+}(DMPS)_2$, for removal of NO from flue gas. Iron(II)$(DMPS)_2$ can bind NO with a very large equilibrium constant, producing a very stable nitrosyl complex that does not react with sulfite/bisulfite ions. Additional information on the NO absorption chemistry of $Fe^{2+}(DMPS)_2$ is needed to predict the NO removal efficiency in full-scale systems, so we investigated the mass transfer and kinetics for the NO complexation process. Two complementary systems were used to investigate the properties of the new additive. The factors that influence the NO absorption kinetics were studied with a double-stirred reactor at 50°C. Using the theory of mass transfer with chemical reaction, the absorption rates and the forward rate constant for NO absorption by $Fe^{2+}(DMPS)_2$ were determined from the measurements. Further studies were conducted with a four-stage turbulent contact absorber. This system was used to investigate the effect of oxygen and obtain parametric data for predictions for the operation of full scale scrubbers.

Double-stirred reactor

We found that the $Fe^{2+}(DMPS)_2$-NO system is strongly influenced by the pH of the solution. Below pH 3, the $Fe^{2+}(DMPS)_2$ system does not enhance NO absorption, presumably because both mercapto groups of DMPS are protonated and the chelate does not bind ferrous ions effectively. The NO absorption rate increases substantially as the pH increases from 4 up to 7, where the maximum NO absorption rate occurs. The NO absorption rates slightly increase when the ratio of Fe^{2+}/DMPS increases from 0.5 to 1.0. Additional Fe^{2+} beyond this ratio does not benefit NO absorption. Moreover, in a real flue gas system with about 5% residual oxygen, the additional uncomplexed Fe^{2+} would be rapidly oxidized.

The reactions between metal chelates and NO should be second order for the forward reaction, *i.e.*, first order in both NO and in metal chelates. To evaluate the forward second-order rate constant of the $Fe^{2+}(DMPS)_2$-NO reaction, the absorption rate of NO was determined with the double-stirred reactor at 50°C. The NO absorption rate increases linearly with the square root of concentration of $Fe^{2+}(DMPS)_2$, which is consistent with the prediction of the pseudo-first-order reaction model. The forward rate constant for the complexation of NO to $Fe^{2+}(DMPS)_2$ was determined to be 1.1×10^8 L/mol s at pH 7.2 and 50°C, about the same as the value for Fe^{2+}(EDTA).

The effect of citrate and sulfite on the NO absorption rate by $Fe^{2+}(DMPS)_2$ solutions was investigated. When there is additional unbound Fe^{2+} in the $Fe^{2+}(DMPS)_2$ system, citrate will improve the NO absorption slightly by forming a ferrous citrate complex which can form a nitrosyl, as in the case of ferrous citrate alone. Without additional uncomplexed Fe^{2+}, the NO absorption rate decreases slightly in the presence of citrate. The NO absorption rate at various sulfite concentrations was measured in a $Fe^{2+}(DMPS)_2$ solution at 50°C. The results indicate that absorption rate decreases as the sulfite concentration increases. In a typical limestone FGD system, there is only a few mM of sulfite ion present, so sulfite will only slightly reduce the NO absorption rate.

Turbulent contact absorber (TCA)

The TCA is a gas absorber containing a bed of low density spheres fluidized by countercurrent flows of gas and liquid. The scrubbing liquor contained 5 wt % limestone and 47 mM iron(II)$(DMPS)_2$. The NO removal efficiency increased linearly with the increase of the liquid:gas ratio (L/G). The NO removal efficiencies are 50% and 70% at L/G values of 60 and 140 gpm/1000 acfm, respectively, while the SO_2 removal efficiencies are above 98%. The liquid film resistance is inversely proportional to the square root of the concentration of iron(II)(L). One way to reduce the liquid film resistance is to increase the iron(II)$(DMPS)_2$ concentration. However, high $Fe^{2+}(DMPS)_2$ concentrations may enhance the problem of chemical loss by entrainment in the solids separated from the scrubbing solution.

The NO removal efficiency was found to be independent of the concentration of NO in flue gas over the range of 100 to 400 ppm. The lack of dependence on gas phase NO concentration is due to the low dissolved NO concentration. It was also found that the NO removal efficiency decreases with the increase of superficial gas velocity from 0.6 to 1.6 m/s. As the gas velocity increases, the gas-liquid contact time decreases from about 1.8 to 0.8 seconds. Consequently, it indicates that an appropriate gas-liquid contact time must be considered for the complexing reaction in a commercial system.

Experiments were conducted to compare the NO removal efficiency between iron(II)$(DMPS)_2$ and iron(II)(EDTA) under similar flue gas scrubber conditions. Initially, EDTA had a higher NO removal efficiency (78%) than DMPS (65%), due to the difference in pH of the solutions. The NO removal efficiency for EDTA dropped dramatically with time, while the DMPS system maintained a stable removal rate. The difference can be attributed to the concentrations of iron(II) since the $Fe^{2+}(DMPS)_2$ is more resistant to oxidation than Fe^{2+}(EDTA) In the presence of 500 ppm NO without O_2, calculations indicate that 10 mM iron(II)$(DMPS)_2$ will form more than 8 mM iron(II)$(DMPS)_2$NO, while 10 mM iron(II)(EDTA) will only form about 3 mM iron(II)(EDTA)NO. The presence of oxygen will also have a larger affect on the iron(II)(EDTA) system than the iron(II)$(DMPS)_2$ system.

From the results of TCA experiments, we made predictions of the performance of a full-scale spray absorber. We calculate that the NO removal efficiency of up to 69% can be achieved. The efficiency increases as the droplet size from the spray nozzles decreases. However, if the droplet size is too small, many of the droplets would be carried up with the flue gas in a counter-current absorber and result in entrainment of the liquor.

Regeneration Studies and Integrated Tests of Ferrous Chelates for NO Removal

Y. Shi, H. Wang, D. Littlejohn, and S-G. Chang

Ferrous chelate additives enhance the solubility of NO in limestone slurries by binding NO to form ferrous nitrosyl complexes. One of the proposed additives, Fe^{2+}(EDTA), is easily oxidized, which causes a decrease in NO removal efficiency. While Fe^{3+}(EDTA) can be reduced to Fe^{2+}(EDTA) by sulfite/bisulfite ions, the regeneration rate is slow. As a result, the Fe^{2+}(EDTA) concentration is low, and adequate NO removal efficiencies cannot be sustained. Prototype systems utilizing electrolytic reduction of Fe^{3+} to counteract the oxidation in the Fe^{2+}(EDTA) system have been developed, but the economics for the processes are not promising.

A new method of regeneration of iron chelates for re-use has been developed, along with a new ligand for ferrous ion: dimercaptopropane sulfonate (DMPS). The DMPS can maintain the iron in the ferrous ion form, resulting in higher NO absorption efficiency. Parametric studies of the absorption efficiency of NO have been conducted and the conditions of the chemical regeneration of ferrous nitrosyl complexes have been investigated. The complexed NO is chemically reduced to ammonia by using iron metal as a reducing agent. Metallic iron is also capable of reducing ferric ion to ferrous ion and reducing oxidized DMPS.

The new ligand and the new regeneration process have been integrated into a complete system and tests have been performed. The integrated process of NO removal by Fe^{2+}(DMPS)$_2$ and regeneration by elemental iron involves several reactions. These reactions may be summarized as follows: (1) absorption of NO by the complex; (2) oxidation of the ferrous ion and DMPS; (3) reduction of the nitrosyl and the oxidized DMPS; and (4) removal of excess ferrous ion by precipitation.

Initially, batch studies were performed to determine the parameters that influence the reduction of the ferrous nitrosyls and oxidized DMPS. We found that iron metal can rapidly reduce complexed NO to ammonium ion. The reduction process is dependent on a number of factors, including reaction time, pH, temperature, reactant concentration, metal surface area, and degree of agitation. Since the reaction is heterogeneous, it is dependent on the contact between the iron particles and the solution. The rate of ferrous ion formation was 2.5 times the rate of ammonium ion formation when both were measured, as would be expected from the reaction stoichiometry. In addition, our experiments indicate that the ligand used in the system also influences the rate of reduction. The reduction of Fe^{2+}(EDTA)(NO) is significantly faster than the reduction of Fe^{2+}(DMPS)$_2$(NO) under identical reaction conditions. Batch studies with oxidized DMPS solutions showed that iron metal can also effectively reduce the disulfide bond. The reaction appears to be somewhat slower than the reduction of the ferrous nitrosyl complex under equivalent conditions.

An integrated system was developed using a turbulent contact absorber (TCA). A scrubbing liquor composed of Fe^{2+}(DMPS)$_2$ and a limestone slurry was circulated through the TCA and a slip stream of the liquor was split off for regeneration. Solids were filtered from the regeneration stream and the filtrate was circulated through a regeneration column containing iron chips. The pH of the regenerated solution was raised to 6-7 to precipitate excess ferrous ion as ferrous hydroxide. The final step of the regeneration was air stripping to remove ammonia produced in the reduction of NO. Make-up limestone was added to the regenerated Fe$^{2+(}$DMPS)$_2$ solution, and it was returned to the scrubbing liquor holding tank for re-use.

Tests of the integrated system were conducted, which consisted of absorption of SO_2 and NO, removal of solids, regeneration of Fe$^{2+(}$DMPS)$_2$, and stripping of ammonia. A steady level of NO removal could be maintained during an entire run. A 16.5 hour test was run at 55°C with 5% oxygen, 105 L/G, 50 mM Fe^{2+}(DMPS)$_2$, 250 ppm NO, and 1500 ppm SO_2. Without any regeneration, the system had an initial NO removal efficiency of 60%, which declined to about 20% after 4 hours. After activating the regeneration system, the NO removal efficiency increased to a level between 43 and 51%. The removal efficiency depended on the operating conditions employed in the regeneration system. We believe that further improvement of the NO removal efficiency can be achieved by increasing the liquor diverted for regeneration, increasing the regeneration time and/or temperature, properly controlling regeneration pH, and by improving the contact between the liquor and the iron metal.

Improved Synthesis of 2,3 Dimercaptopropane Sulfonate

K.W. Huang and S.-G. Chang

We have found that aqueous ferrous ion complexes of 2, 3-dimercapto-1-propane sulfonate (DMPS) are very effective in removing NO from flue gas. Currently, DMPS is only commercially available in reagent grade and in limited quantities. For this technology to be commercialized, DMPS must be available in large quantities and at low cost. An inexpensive synthesis method for industrial grade DMPS is needed for this NO removal process to be commercialized.

We have developed a synthesis procedure for DMPS that is a significant improvement over the standard literature procedure developed by Petraikin. The new process produces DMPS at higher yield and with less expense associated with byproduct separation. In our procedure, DMPS is synthesized based on the reactions shown in the Figure.

In the first step of the synthesis procedure, we use a reactant ratio of 1.2:1 for allyl bromide and sodium sulfite instead of the 1:1.1 ratio used in the literature method. With this procedure, sodium sulfite does not remain in the reaction mixture after the first step. After cooling, the small amount of residual allyl bromide precipitates and is separated from the solution with a separatory funnel. In commercial applications, the remaining allyl bromide could be reused. This prevents the redox reaction between sodium sulfite and bromine from occurring in the second step of the literature synthetic procedure.

The second step of our procedure involves the reaction of allyl sulfonate with bromine. The reaction was carried out at several temperatures (10, 23, and 35°C), and the reactants and products were measured by high performance liquid chromatography (HPLC). Over the temperature range studied, all of the allyl sulfonate was consumed to form dibromopropane sulfonate. Therefore, no byproducts are formed when the reaction is carried out over the temperature range studied. In an industrial synthesis, DMPS can be produced without cooling the reaction mixture, simplifying the system and lowering the cost.

The third and final step of the synthesis was carried out by reacting aqueous dibromopropane sulfonate (I) with sodium hydrosulfide (II). Factors that affect this reaction include the reactant mole ratio, the reaction time and temperature, and the concentration of dibromopropane sulfonate. We used HPLC to analyze the reaction mixtures prepared at 50°C. We found that by using a I:II mole ratio of 1:4 or less, we could achieve >96% yield after 5 min. reaction time. For comparison, the literature method of Petraikin achieved <52% yield using a I:II mole ratio of 1:2.5.

The dependence of this step on temperature and concentration was also investigated. While >96% of the dibromopropane sulfonate reacted in 5 min. at 50°C, 89.3% reacted in the same time at 35°C. When the dibromopropane sulfonate concentration was changed from 25% to 12%, the yield of DMPS dropped from >96% to <58% after 5 minutes reaction time. However, when the mix with the lower reactant concentration was allowed to react for 60 min., the yield increased to 92.4%

In summary, our improved synthetic procedure increases the overall yield of DMPS from 30% to 69%. The process we have outlined here will provide a means to prepare DMPS inexpensively on an industrial scale.

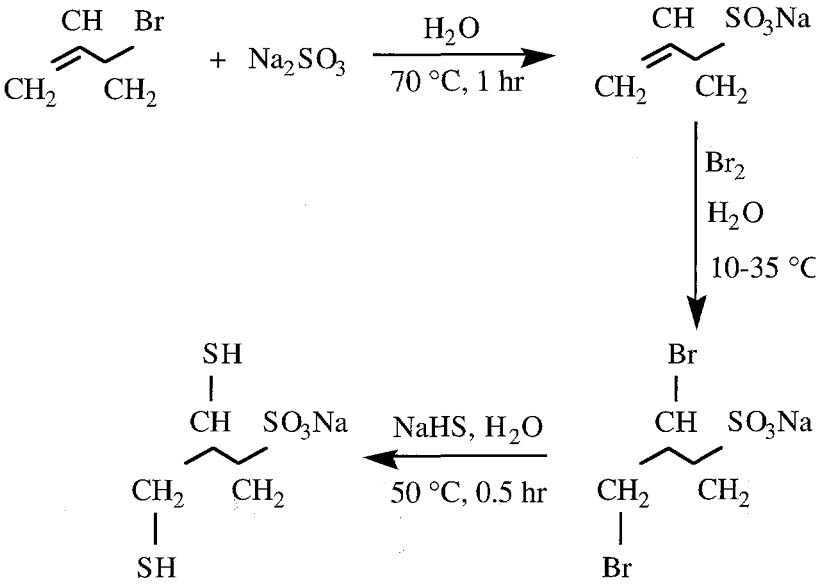

Figure. *Synthesis of 2,3-dimercapto-1-propane sulfonate (DMPS) in new process that increases overall yield of DMPS from 30% to 69%.*

Catalytic Reduction of Sulfur Dioxide to Elemental Sulfur

Y. Jin, Q. Yu, and S.-G. Chang

Several regenerable processes for flue-gas desulfurization (FGD) have been commercialized or are under development. In these processes, sulfur dioxide in flue gas is first absorbed into an alkaline solution or adsorbed on a solid substrate. It is subsequently desorbed to produce a stream of concentrated sulfur dioxide, which is then converted into elemental sulfur for storage, transport, or later conversion to other compounds. In these processes, either methane ($H_2/CO = 3$), or synthesis gas derived from coal ($H_2/CO = 0.3$ to 1.0), can be used to reduce sulfur dioxide to elemental sulfur at elevated temperatures, according to the following reactions:

$$2SO_2 + CH_4 \rightarrow S_2 + CO_2 + H_2O \tag{1}$$

$$2\,SO_2 + 3\,H_2 + CO \rightarrow S_2 + CO_2 + 3\,H_2O \tag{2}$$

$$7\,SO_2 + 6\,H_2 + 8\,CO \rightarrow 3.5\,S_2 + 8\,CO_2 + 6\,H_2O \tag{3}$$

Catalysts are generally used to facilitate these reactions. In addition to elemental sulfur, these reactions may produce several undesirable byproducts. These include hydrogen sulfide, carbonyl sulfide, carbon disulfide, and elemental carbon. Considerable research has been carried out to develop catalysts that minimize the formation of byproducts. If byproduct production is negligible, then additional treatment to remove them is unnecessary. We have developed a promising new catalyst that maximizes yield of elemental sulfur and minimizes byproduct production.

We evaluated cobalt oxides on several types of supports for their ability to reduce sulfur dioxide with methane. The catalyst-support combinations were tested at 740 to 820°C. They ranked in the following order with respect to elemental sulfur yield (Y_{S2}): $Co_3O_4/\gamma\text{-}Al_2O_3 > Co_3O_4/SiO_2 > Co_3O_4/$Molecular Sieve 13X > $Co_3O_4/$ Molecular Sieve 5A. The results obtained for a stoichiometric mole ratio of 2:1 of sulfur dioxide to methane in the feed gas are shown (Table).

The yield of elemental sulfur reached a maximum of 87.5% at a space velocity of 5,000/h and a temperature of 840°C. X-ray diffraction results revealed that the catalyst was composed of Co_3O_4 and $\gamma\text{-}Al_2O_3$ before the reaction, and changed to structures of $\beta\text{-}COS_{1.035}$, COS_2, Co_3O_4, and $\gamma\text{-}Al_2O_3$ after the reaction.

An iron-based mixed oxide catalyst (Cat-S) has been developed for reduction of SO_2 by synthesis gas. The catalyst can achieve high SO_2 conversion efficiency and high elemental sulfur selectivity, and is capable of achieving reduction of SO_2 in a single stage reactor. A lifetime (1080 hours) test was performed on the catalyst on 30-40 mesh alumina support. The test was conducted at 480°C and 10,000/h space velocity. The activity of the catalyst remained very stable during the entire period of the test. The yield of sulfur was in excess of 94%. There was little variation with time in the Y_{H2S} and Y_{COS}, as well as SO_2 conversion efficiency. A good mass balance of sulfur and carbon was obtained in the measurements.

We have found that when impregnated on alumina granules 3 mm in diameter × 5 mm long, this catalyst material can achieve 96.2% and 97.8% yield of elemental sulfur at 540°C and 560°C, respectively, at a space velocity of 2100/h. The catalyst requires only a stoichiometric amount of synthesis gas for SO_2 reduction.

The effect of the commonly found byproducts and contaminants H_2S, COS and H_2O on the Cat-S material was investigated for reduction of SO_2 by syngas. The addition of either 10% H_2S or 10% COS, or a combination of 10% H_2S and 10% COS to the feed gas did not affect the yield of S_2. The measurements were made under the following conditions: 420°C-480°C, 10,000/h space velocity, H_2/CO ratio of 0.4, $(CO+H_2)/SO_2$ ratio of 2.0, and 30-40 mesh catalyst support. In the presence of up to 20% H_2O, the Y_{COS} increased with decreasing reaction temperature below 440°C. The yield of S_2 also decreased with decreasing reaction temperature. However, there was no observable effect of water above 440°C. The yield of H_2S remained relatively unchanged between 380°C and 600°C.

We are continuing our investigation of the new catalysts. We are currently studying the conversion efficiency at lower (0.3 - 10%) SO_2 concentrations and the effect of oxygen on the reduction process. We believe the new materials are very promising, and have the potential to be incorporated into a more efficient, cost-effective regenerable flue gas desulfurization process.

Table. *Results of evaluating cobalt oxides for their ability to reduce SO_2 with methane.*

	Temperature (°C)	**SO_2 Conversion Efficiency (%)**	**Selectivity to Elemental Sulfur (%)**
Test 1	780	98.7	80.0
Test 2	820	98.7	87.9

NO_2 Reactions in Aqueous Flue-Gas Scrubbing Systems

D. Littlejohn

Flue gases from coal-fired power plants generally contain hundreds of ppm of nitrogen oxides. The nitrogen oxides are generally composed of at least 90% nitric oxide, with the remainder existing as nitrogen dioxide. Nitric oxide is only slightly soluble in water, and ferrous ion-based additives are being developed to enhance its solubility. Nitrogen dioxide is substantially more soluble than nitric oxide. Some processes, such as the LBNL PhoSNOX process, can convert nitric oxide into nitrogen dioxide in the flue gas stream. An understanding of the reactions of nitrogen dioxide with additives and dissolved gases in scrubbing solutions is needed to understand aqueous scrubber chemistry and to properly design scrubbing systems.

Nitrogen dioxide will react with aqueous scrubbing solutions. The primary reaction in aqueous systems is that of reactive dissolution in water:

$$2\,NO_2 + H_2O \rightarrow 2\,H^+ + NO_2^- + NO_3^- \qquad (1)$$

The reaction of nitrogen dioxide with dissolved sulfur dioxide was studied previously,

$$NO_2 + SO_3^{2-} \rightarrow NO_2^- + SO_3^- \qquad (2)$$

The formation of sulfite radical can create conditions for a free radical chain reaction which can oxidize many sulfite ions in the presence of oxygen.

NO_2 can also oxidize other species in solution. For example, it will oxidize ferrous ion to ferric ion in the absence of oxygen. An electron transfer reaction occurs:

$$NO_2 + Fe^{2+} \rightarrow NO_2^- + Fe^{3+} \qquad (3)$$

The reaction was studied by measuring the reaction products. Nitrite ion was determined by ion chromatography and ferrous ion was determined by 1,10 phenanthroline colorimetry. The reaction displays first order dependence on the gas phase nitrogen dioxide concentration and on ferrous ion concentration. The reaction rate was compared with that of NO_2 + sulfite reaction. The measurements done so far indicate that rate constant of the $NO_2 + Fe^{2+}$ reaction is about $1/6$ of that for the $NO_2 + SO_3^{2-}/HSO_3^-$ reaction. Therefore, in scrubbing solutions where the S(IV) concentration is in excess of the ferrous ion concentration, the sulfite/bisulfite ion should effectively protect the ferrous ion from oxidation. It has been reported that nitrogen dioxide will bind with ferrous ion complexes prior to oxidation of the ferrous ion, which could interfere with the removal of nitric oxide by ferrous chelates under certain conditions. Nitrogen dioxide is generally a minor component of flue gases with which ferrous chelate solutions are used, and oxidation of ferrous ion by residual oxygen will be much more important than oxidation by nitrogen dioxide.

Thiosulfate is an additive used in some aqueous scrubbing processes as an oxidation inhibitor. It can also react with nitrogen dioxide by electron transfer.

$$NO_2 + S_2O_3^{2-} \rightarrow NO_2^- + S_2O_3^- \qquad (4)$$

The thiosulfate radical formed can dimerize to form tetrathionate ($S_4O_6^{2-}$), which we have observed in solutions of thiosulfate exposed to nitrogen dioxide. The reaction of nitrogen dioxide with thiosulfate is substantially slower than the reaction with sulfite ion.

Nitrogen dioxide is a very reactive compound and its interactions with aqueous solutions can be quite complicated. Our studies should improve the understanding of wet flue gas scrubber chemistry. It should be noted that some of the reactions of nitrogen dioxide that are described here are also important in the chemistry of aqueous aerosols in the atmosphere.

Combustion

Combustion Fluid Mechanics

R.K. Cheng, I.G. Shepherd, B. Bedát, D. Yegian, and L. Talbot

Turbulent combustion takes place in all heat and power generating systems. Its most important role is to increase the burning rate and volumetric power density. Intense turbulence, however, also influences the combustion reaction rates and has a direct effect on emission, ignition, and extinction. Therefore, research and development of modern combustion systems for power generation, waste treatment, and material synthesis must rely on a fundamental understanding of the physical effects of turbulence on combustion. Such knowledge is key to successful development of theoretical and computational models that can be used as design tools.

The objective of our research is to investigate the interaction and coupling between turbulence and combustion. These processes are complex and involve scalar and velocity fluctuations with time and length scales spanning several orders of magnitudes. The burner and flame geometries also have profound effects. Our approach is to investigate laboratory flames with geometries that are designed to facilitate direct comparison with numerical modeling and theoretical analysis. These burners are also amenable to detailed interrogation by laser diagnostics and allow systematic independent variations of turbulence intensities, flow conditions, and mixtures compositions.

The main focus of our experiment has been on investigating flames with moderate turbulence intensity. This type of combustion where chemical reaction rates are much faster than turbulence mixing occurs in most small to medium combustion systems such as residential appliances and automobile engines at idling condition. The turbulent burning rate can be evaluated by determining how turbulence wrinkles the flame front. The flame front topology (i.e., the degree of flame wrinkling) relates directly to turbulence scales and intensities. Recently we have extended the scope of the experiments to include flames with intense turbulence. These flames are closer to the burning conditions in larger power generating systems. Intense turbulence can affect chemical reaction rates which may lead to a reduction of burning rate, intermittent flame quenching and re-ignition, and ultimately flame extinction.

In practice, turbulent flames burn in combustion chambers of different sizes and geometries. These differences changes the boundary conditions upstream and downstream of the flame. Therefore, it is important to simulate these differences in the laboratory. We have thus far developed five laboratory flame configurations. Our burners are designed to operate under a wide range of conditions so that changes in flame characteristics can be correlated to different turbulence intensities and mixture equivalence ratios. Their configurations provide experimental data that can be compared with statistical one-dimensional (1-D) and deterministic two-dimensional (2-D) models, and three-dimensional (3-D) direct numerical simulations.

To capture the rapid changes of turbulent flames, our experimental methods emphasize laser techniques with high spatial and temporal resolutions. To characterize the statistical moments and correlations at a point within the flame, we use laser Doppler anemometry (LDA) for measuring velocity fluctuation and laser-induced Rayleigh scattering for measuring scalar fluctuations (i.e., gas density, reaction progress variable). A simple method we have developed for determining the flame wrinkle scales is laser-induced Mie scattering from silicone-oil aerosol (MSOD). This technique is also used in conjunction with a laser sheet to render 2-D imaging of the flame wrinkle geometry at high-speed (i.e. to-

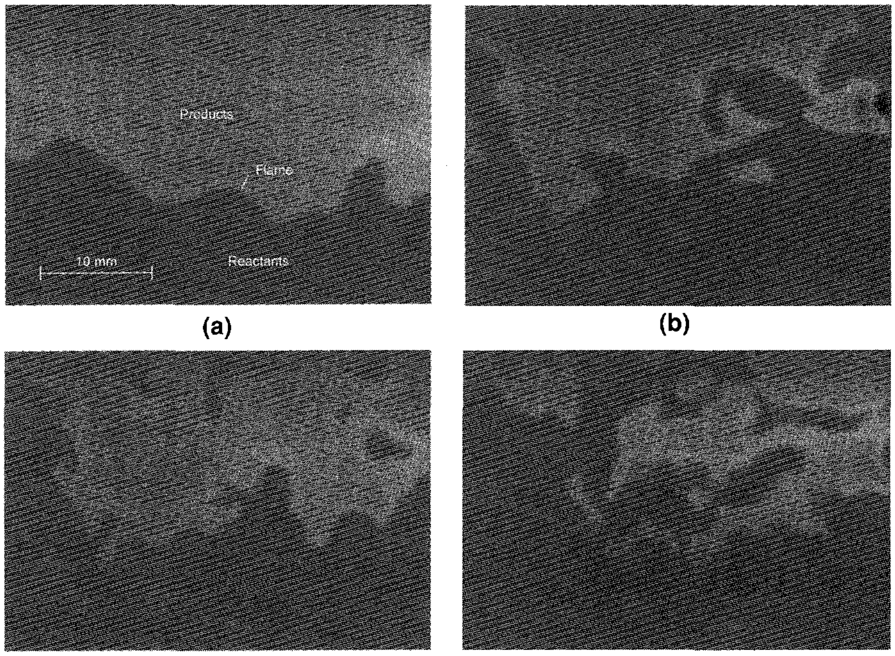

(a) (b)

(c) (d)

Figure 1. *Planar Laser Induced Fluorescence (PLIF) images of OH radicals in four premixed turbulent flames with increasing turbulence intensity u′. OH radicals are produced in the hot products and they fluoresce and thus appear bright on these images. The boundaries between the bright and dark regions is the flame. Turbulence fluctuations u′ are (a) 0.5 m/s (b) 0.89 m/s (c) 1.3 m/s and (d) 1.7 m/s.*

mography). Other imaging method includes laser schlieren to infer overall flame behavior. Our latest 2-D diagnostic development is Planar Laser-Induced Fluorescence (PLIF) to infer the internal turbulent flame structure. Our PLIF system is based on a dye laser pumped by a Nd-YAG laser. PLIF is essential for us to investigate changes that occur at intense turbulence. All our imaging diagnostics are controlled by a PC and use conventional or intensified video cameras.

Flame propagation in intense turbulence

The development of a burner for investigating premixed turbulent flames propagating in intense isotropic turbulence has provided the means to vary the turbulent intensities of our experiments from laminar to the conditions of typical turbines of up to 20%. With the implementation of the PLIF technique, we embarked on a program to compare and characterize turbulent flame structures to test and verify theoretical assumptions regarding the differences between flames classified as wrinkled laminar flame (under moderate turbulence), corrugated flames, and flames with distributed reaction zones (under intense turbulence).

Figure 1 shows PLIF images of hydroxide radicals (OH) in four flames with increasing turbulence intensities. To capture these images, the pulsed-dye laser beam was formed into a sheet 30 mm high and 0.5 mm thick. This laser sheet dissected the turbulent flames and the ultraviolet fluorescence radiation from the OH radicals present only in the hot combustion products was recorded by an intensified UV camera. The boundary between the bright product region where OH radicals were present and the dark reactants region is the thin flame front. From Figure 1(a) it can be seen that under moderate turbulence, the flame is slightly wrinkled and typical size of these wrinkles are about 10 mm. The features of the flame wrinkles change drastically when turbulence intensity is increased. Smaller flame wrinkles begin to appear and the flame shape is much more irregular. At the higher turbulence level we have investigated (velocity fluctuations approaching 1.5 m/s), flame pockets and large excursions of the flame boundary are typical characteristics. According to prevailing theory, flames shown in Figures 1(b) to 1(d) are described as flames with "distributed reaction zones." That is, their flame fronts should have evolved from thin reaction zones to more diffused and broadened regions. Our OH PLIF images seem to contradict this theoretical notion as the flame boundary as shown by the increase in OH concentration remains sharp and well defined. A more diffused flame boundary is found only sporadically (Figures 1(c) and 1(d)).

Though these PLIF images have demonstrated vividly the drastic changes that occur when flames are subjected to increasing turbulence intensities, quantifying these changes will require extensive image processing and development of analysis methods. As a start, we have obtained at least six to twelve images for each condition and used them to develop the analysis for quantifying the flame wrinkle scales. A more challenging task will be to develop the OH PLIF technique for measuring the local reaction rate on the flame fronts.

Coupling of premixed flames with gravity.

Buoyancy plays an important role in open flames. The rising hot plume affects the flow pattern within the flame and in its surrounding environment. Buoyancy can ventilate and maintain stable burning or it can induce flame instability. Our research on flame/buoyancy coupling relates to the dynamic interaction between the flame and its surrounding environment. For laminar and mildly turbulent flames, buoyancy controls the flow pattern, flame shape, flame stability, and burning rate. The extent of these effects differs depending on burner configuration, flow momentum, and flame intensity. Our goal is to characterize these effects and determine at what point they are insignificant. Key to our study is the investigation of microgravity (mg) flames, that is flame burning in a low gravity environment. These mg experiments provide vital information to reconcile the differences between flames in normal gravity (+g, flame pointing upward) and reverse gravity (-g, flame pointing downward). The mg experiments are performed using two facilities at the NASA Lewis Research Center in Cleveland. As mg experiments are much more difficult to conduct than laboratory experiments, the diagnostics we can use are also limited. The schlieren imaging technique selected for our work is a convenient and simple method that shows changes in flame shape.

In preparation for our next mg experiments, we have determined in the laboratory the effects of buoyancy on the flame stabilization limits for our two mg flame configurations. During the course of our investigation of -g flames, we discovered the existence of buoyancy-stabilized laminar flames (Figure 2). These flames are very stable, relatively flat, and detached from the burner exit. Their stabilization mechanism is independent of flow recirculation or external means. The basic im-

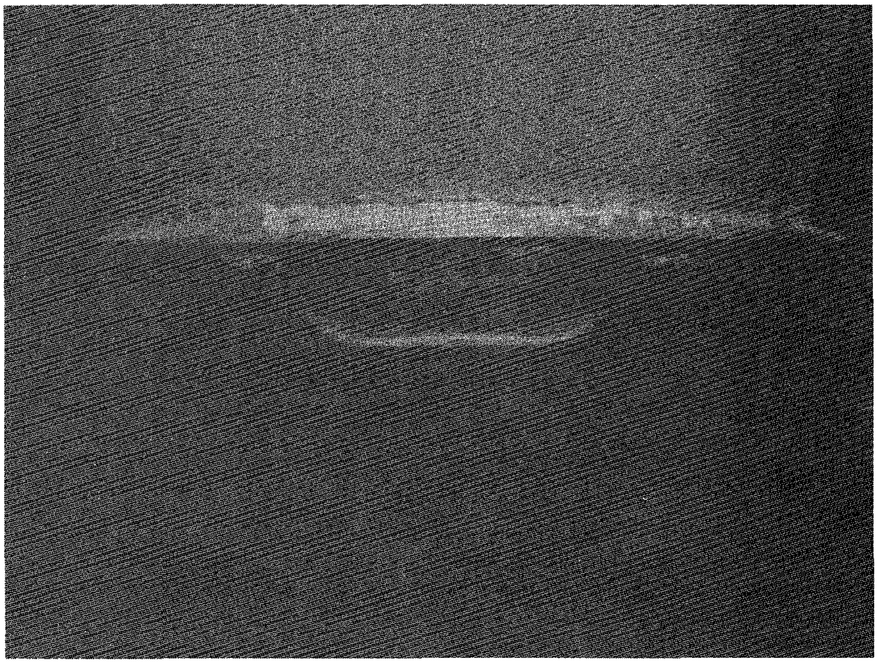

Figure 2. *When the burner is turned upside-down, upward buoyancy forces of the hot combustion products counteract the flow exiting the burner to produce a stable flat flame.*

plication is that buoyancy in the hot products produces the appropriate flowfield that enables the flame to propagate steadily into the reactant stream coming out of the burner.

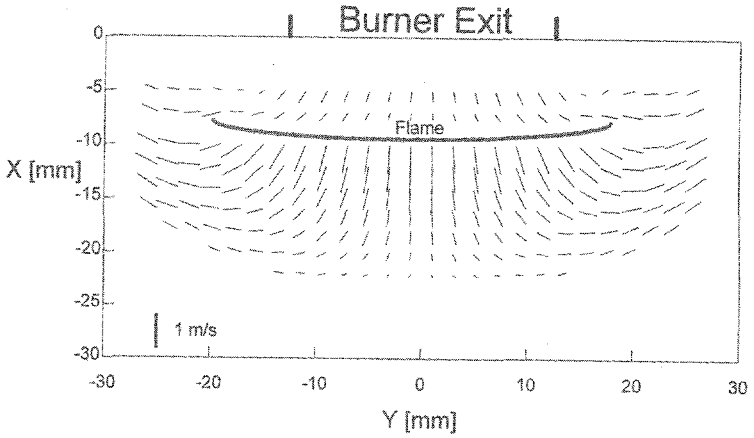

Figure 3. *Velocity vectors obtained in a buoyancy-stabilized laminar premixed flame (see Fig. 2) with exit velocity $u = 0.54$ m/s and methane-air equivalence ratio $\phi = 0.725$.*

This unique flame configuration is of fundamental importance to characterizing flame/buoyancy coupling because it encapsulates the essential physics of the problem. As shown by the flow vectors obtained by LDA (Figure 3), buoyancy in the hot products produces flow divergence. The divergence effect from downstream of the flame zones affects the mean flame features upstream primarily through changes in the mean pressure field. This seems to be the important mechanism through which buoyancy influences premixed flame propagation. As these buoyancy-stabilized flames are not influenced by flame geometry or means of flame stabilization, they are ideal for investigating how buoyancy interacts with flow momentum, what effects it has upstream and what are the relevant parameters to describe the interacting processes. Such knowledge would be very useful for characterizing the effects of buoyancy on more complex turbulent flames. We have carried out a detailed study of these buoyancy-stabilized flat flames. First, the conditions under which they can be generated were determined. Next, laser Doppler anemometry was used to measure the 2-D velocities in the flowfields. These velocity data have been used in an analysis to characterize the buoyancy/flow balance in the flowfields.

Technology transfer

As a necessary part of fundamental rsearch, we routinely design laboratory burners that allow the study of turbulent flames under a wide range of conditions to facilitate systematic variation of experimental parameters. Some of these burners are significant to support development of theoretical works. Others can be used in practical applications. Recently, two of our burners were recognized as having potential for commercialization. Their main attribute is their ability to support lean (excess air) premixed combustion that produces very low levels of oxides of nitrogen (NO_x). NO_x emissions from combustion is the major cause of smog and ozone layer depletion. Proposed air quality regulations would limit NO_x emissions to several times lower than the current standard. Manufacturers are seeking economical ways to meet these new standards.

Once generated, NO_x is relatively difficult to remove. In conventional burners, NO_x is generated at a high level and removed by the use of catalyst and other techniques. Rather than a removal technique, lean combustion minimizes the formation of NO_x by lowering combustion temperature. The reason why lean combustion is not commonly used is that it blows off easily. Our two burners solve the blow-off problem by relatively simple means. The first uses a ring flame stabilizer mounted inside the burner tube. The second uses weak swirl to stabilize the flame aerodynamically.

The weak-swirl burner is currently being tested in our laboratory for use in water heaters. This work is a collaboration between LBNL and Teledyne Laars of Moorpark, California. The picture shows the weak-swirl-burner mounted in a Teledyne Laars Telstar Spa Heater. This laboratory test station is a working water heater system with output power between 15 to 21 KW. A PC is used to monitor the thermal efficiency of the system and record the emissions of NO_x and CO. The results we have obtained are quite gratifying. As shown in Figure 4, we found that the Telstar/weak-swirl-

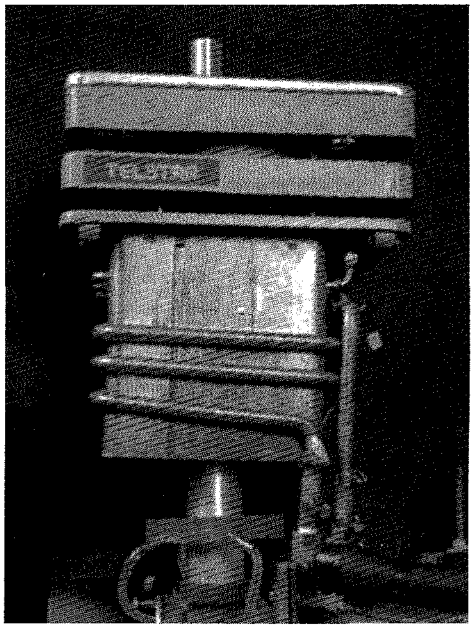

Figure 4. *Laboratory testing station with the Weak-Swirl Burner incorporated into a Telstar spa heat exchanger from Teledyne Laars.*

burner system meets the proposed "low" NO_x (50 ppm) and "ultra low" NO_x (25 ppm) limits without sacrificing efficiency. The test results will be use to guide the design of a prototype for testing at Teledyne Laars.

Planned activities

We plan to develop OH PLIF technique for quantifying the local reaction rate in flames with intense turbulence. The experimental conditions will be extended to explore if turbulence can cause local flame quenching.

The investigation of the flame/gravity coupling will focus on the development of quantitative diagnostics suitable for use in the microgravity facilities at NASA-Lewis, Research Center.

Work planned for the CRADA with Teledyne-Laars will include the design of a different air or mechanical swirler appropriate for water heaters of various sizes. Also planned is testing of the operation with burners positioned side by side to investigate if they interact.

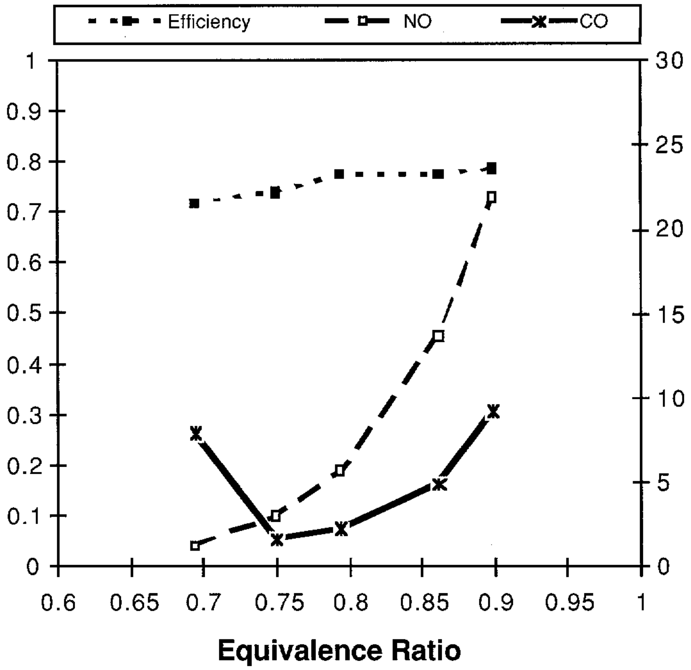

Figure 5. *Test results from the WSB-Telstar heater for varying excess air ratios with a constant firing rate of 18 kW. Ultra-low* NO_x*(<25 ppm) attained for excess air greater than 10%.*

Combustion Chemistry

J. Chang and N.J. Brown

Theoretical modeling of combustion involves a multilevel approach that encompasses fluid mechanical models of flames at the macroscopic level to dynamical models of chemical reactions at the microscopic level. Our research effort is focused on the fundamental chemistry aspect of combustion modeling and, in the past year, has proceeded along two fronts. The major component of our effort has been a continuation of work from previous years in attempting to elucidate the subtle relationship between inaccuracies in the potential energy surface (PES) and its effects on the molecular dynamics. This work is important for developing a reliable theoretical model that can explain all the experimental observations. We conducted this investigation using the tools of quantum functional sensitivity analysis (QFSA). In a second effort, we continued a collaboration with scientists at Sandia National Laboratory (Livermore, California) to calculate reaction rate constants via real time Monte Carlo path integrals, in particular employing massively parallel computers. The details of our progress in these two fronts are described below.

The question of how errors in the PES manifest themselves in dynamical observables has been a long standing research problem in our group. This past year, we applied the technique of QFSA to study both the $F + H_2 \rightarrow HF + H$ and the $D + H_2 \rightarrow HD + H$ reactions. The $F + H_2$ reaction is one of the most extensively studied elementary chemical reactions in recent history because of its prominent role in developing theories of chemical reactivity and because of the suite of challenges it has provided to both theory and experiment. The crossed molecular beam experiments from the research group of Y.T. Lee yielded vibrationally state-resolved differential cross sections and vibrational branching ratios which corroborated previous experimental observations of the highly inverted HF population. For the energy range of their investigation, the most highly populated state was found to be $v' = 2$ followed by $v' = 3$ and then $v' = 1$. On the theoretical side, quantum dynamics calculations yielded mostly $v' = 3$ followed by $v' = 2$ with very small $v' = 0$ and 1 population. This discrepancy with experiment was traced back to deficiencies in the PES, and it sparked many new PES developments in several research groups.

The current method of PES refinement is a complex iterative procedure of fitting a global PES, often involving new, high level *ab initio* quantum chemistry calculations, followed by accurate quantum dynamics calculations and comparisons with experiment. This is a time-consuming and expensive procedure often requiring many years of research. With the addition of sensitivity information, as shown in the Figure, one can considerably simplify the PES refinement effort. The sensitivity contour map shows several regions of the PES where one can make modifications to increase population into $v' = 2$ and decrease population into $v' = 3$. The positive sensitivity contours correspond to regions where the observable increases when the potential is increased and conversely for the negative sensitivities. Sensitivity maps also provide important information for the global PES refitting effort. Regions of largest sensitivities point to locations in configuration space where more *ab initio* points should be calculated, and where one should place the highest weight in the least-squares fit of the global PES.

For the $D + H_2$ reaction, we calculated sensitivities of the rate constant to small variations in the PES. Very accurate potential surfaces for this reaction already exist and one can obtain excellent agreement with experiment for many of the calculated observables. At the high temperatures seen in combustion, however, there is still some disagreement between theory and experiment. The calculated rate constant at 1500 K is about 30% below the experimentally observed rate constant. The explanation proposed for this discrepancy (barring experimental error) is that some deficiencies remain in the fit to the high-energy regions of the PES. The sensitivity information we provide should be useful in a refit of the PES which eliminates these remaining discrepancies.

In our Sandia collaboration, we are investigating the feasibility of using massively parallel computers to evaluate real time Monte Carlo path integrals. In the past, attempts at direct evaluation of the path integrals arising from the flux-flux autocorrelation function formulation of reaction rate theory have failed because the highly oscillatory integrands precluded convergence on conventional supercomputers. We are thus querying whether or not a thousandfold increase in computing power is sufficient to converge the path integrals. If this approach succeeds, we will have a powerful method for calculating rate constants that is applicable to a wide variety of chemical reactions. We are currently testing the methodology for an H-atom tunneling through a simple one-dimensional Eckart barrier. A parallel version of the code has been developed which shows excellent scalability with the number of processors.

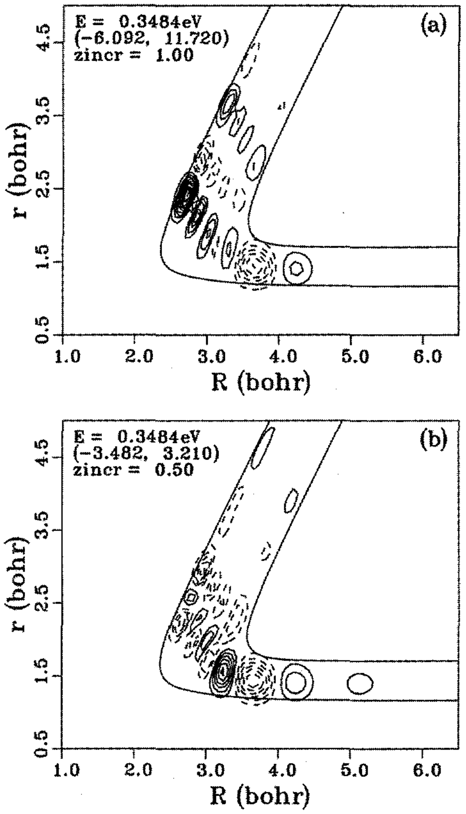

Figure. *Sensitivity maps for the zero partial wave F + H_2 reaction probability from the initial v = 0, j= 0 state to the product vibrational manifolds (a) v¢ = 2 and (b) v¢ = 3 at the energy E = 0.3484 eV. Contour values are drawn in increments of zincr shown on the plots. Positive contours are represented by solid lines; negative contours, by dashed lines. Zero contour line is omitted. Numbers in parentheses represent minimum and maximum sensitivity values on an 80 × 65 rectangular grid. All sensitivity contour values are given in units of $eV^{-1}bohr^{-6}$. The 0.3484 eV equipotential of the potential energy surface is shown by solid heavy lines.*

For future work, we plan to extend our sensitivity analysis work to other chemical reactions. Both the F + H_2 and H + O_2 reactions are currently mired in controversy with the blunt of the blame being placed on inaccuracies in the PES. We believe that QFSA can provide feedback information to quantum chemists in their PES refinement efforts. For the rate coefficient work, several methods are under investigation. The main thrust of these investigations is to eliminate the need for state-to-state reactive scattering calculations, and thus to considerably simplify the calculations without sacrificing accuracy. As the method of choice emerges, concomitant development in sensitivity analysis will be required.

Reference

Chang J, Brown NJ. Comparison of the quantum dynamics and sensitivity analysis for different isotopomers of the H + H_2 reaction. *Journal of Chemical Physics* 1995; 103: 4097.

Thermal Destruction of Toxic Compounds

D. Lucas, R.F. Sawyer, C.P. Koshland, S.G. Buckley, B.S. Higgins, A. Wilson, H. Clack, J. DuBois, and L. Sgro

We continue to study how chemical species, especially metals and chlorinated hydrocarbons, react when they are heated. High temperature reactions are important not only for destroying wastes using incineration, but also for chemical synthesis, oil and gas processing, and other remediation efforts. The goals of our research are to gain a fundamental understanding of the chemical processes that occur when metals and chlorinated hydrocarbons are destroyed thermally, study new ways to enhance the destruction of these compounds, and to develop new diagnostic methods for the measurement of these species and their byproducts.

Detecting metals at high temperatures

We have used excimer laser fragmentation fluorescence spectroscopy (ELFFS) to study metal species in flames and in the post-flame gases. The method uses one or two lasers to detect metal atoms or fragments produced when 193 nm light from an excimer laser fragments metal compounds. The single laser ELFFS technique can measure Ba, Cr, Mn, Ni, Pb, and Tl at sub-parts-per-million levels in post-combustion gases simultaneously and without background interferences, as shown in Figure 1 (next page). The signal is linear with concentration of the metal and with the incident laser power. Changes in the quenching of the excited states are insignificant over the range of conditions typically found in combustion exhausts.

The signal depends on the surface area of particles present, which we use to detect the onset of nucleation in Pb species in the 600-750 K temperature region. The method has also been applied to laboratory flames, where we detect atoms formed at the high temperatures in the flame zone. These measurements show that ELFFS can be a valuable tool for the study of metal chemistry in flames, as well an emissions monitor capable of meeting the demands of current and pending regulations.

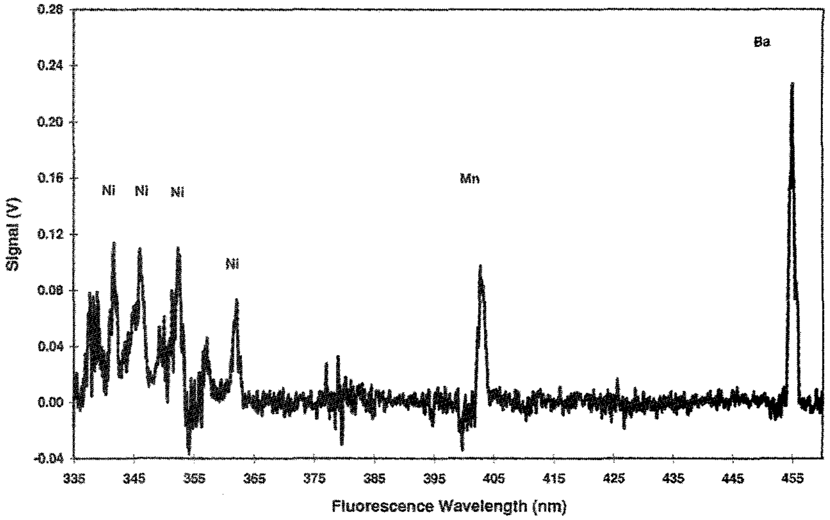

Figure. *Post-flame single-laser ELFFS of mixture of $BaCl_2$, $NiCl_2$, and $MnCl_2$ injected at 3 ppm each into the standard flat flame.*

Flow reactor studies

We have expanded our chlorinated hydrocarbon studies to include methylene chloride, chloroform, and chlorobenzene. Benzene was also studied as the prototypical aromatic compound. Results using a new, vertical reactor allow us to change oxygen content, temperature, and residence time independently. We have determined reaction pathways and examined how trace levels of toxic byproducts can be formed. Detailed chemical kinetic modeling is used to identify reactions which are crucial in these systems, and to suggest control strategies which can be tested experimentally.

Packed-bed reactors

Thermatrix, Inc. and LBNL have continued studying a commercial packed-bed reactor used to destroy trace amounts of organic species. We are now examining if and how dioxins and furans are formed in environments where no flame is present, and exploring methods to reduce the levels produced. We have modified standard EPA methods for collecting these species to avoid complications produced by high pH exhausts when large amounts of acid gases are formed in the destruction process.

References

Vitovec W, Koshland CP, Lucas D, Sawyer RF. The destruction of methylene chloride in lean post-flame conditions. *Combustion and Flame* (in press).

Thomson M, Lucas D, Koshland CP, Sawyer R F. Reducing hazardous waste incinerator emissions through blending. *Hazardous Waste and Hazardous Materials* (in press).

Martin RJ, Wilson A, Vitovec W, Koshland CP, Lucas D. On-line detection of chlorinated organics in a packed bed oxidizer. Presented at 4th International Congress on Toxic Combustion Byproducts, June 1995, Berkeley, California.

Atmospheric Processes

Organic Aerosols in Tropical Tradewinds

T. Novakov, C. E. Corrigan, O. Rosario, and O. Mayol*

We have analyzed sub-0.6-micrometer aerosol samples collected at Cape San Juan lighthouse (about 50 m from the ocean) located on the easternmost edge of Puerto Rico. Samples were collected when the wind direction was from the east to northeast sector. Under these conditions, no obvious nearby upwind anthropogenic sources should impact the site, virtually assuring that the collected aerosol is representative of tropical marine tradewinds.

Measurement results are as follows: (1) Sub-0.6-μm organic aerosol mass concentrations (average about 500-600 ng/m^3) significantly exceed sulfate concentrations (average about 250 ng/m^3). (2) This organic aerosol material is water soluble. (3) The aerosol samples did not show any coloration due to mineral dust or black carbon; maximum black carbon concentrations are about 30 ng m^3. (4) Seasalt particles are an insignificant source of organic aerosols. (5) The thermal volatility of trade wind organic aerosol material is similar to that of ammonium sulfate.

Because the samples were collected under tradewind conditions, we postulate that either the aerosols are generated in upwind, perhaps continental, locations and carried to the site by the trade winds, or they are produced by gas-to-particle conversion from precursors originating in oceanic air masses. The following reasoning appears to favor the second alternative:

- Because black carbon is a tracer for combustion, its virtual absence suggests that combustion is not the main source of the (sub-0.6 μm) aerosol at this site.
- Thermal evolved gas analyses show that the thermograms of trade wind aerosol organics are radically different from those observed in continental combustion–influenced regions.
- Because the organic aerosol material is water soluble, it is unlikely that such water-soluble aerosols will reach the

sampling site by long-range transport.

- Sulfate concentrations are within the range of concentrations expected from natural marine sources.

These observations do not support the view that long-range transport of anthropogenic combustion aerosols is a significant contributor to the organic trade wind aerosols. The gas-to-particle conversion alternative seems to be suggested by the following:

- The presence of significant concentrations of semivolatile aerosol organic species and the relative volatility of filterable particulate organics suggests fresh aerosol rather than aged.
- In contrast to sulfate, organic aerosol mass concentrations are higher during daytime than at night, possibly indicating the production of organic aerosols by photochemical reactions. (Warm temperatures and intense UV radiation are favorable for photochemistry.)
- Significant concentrations of gaseous organics adsorbed on the filter matrix suggest the presence of substantial concentrations of total gaseous organic compounds; some of these may be precursors of organic aerosols.

This evidence, although speculative, tends to support the view of *in-situ* formation of organic aerosols by gas-to-particle conversion in marine atmospheres.

The fact that marine organic aerosols are water soluble is consistent with our earlier findings, which show that organic aerosol material is a major contributor to both total aerosol (CN) and cloud condensation nuclei (CCN) number concentrations. These findings, if confirmed by more measurements at the present site and other oceanic sites, should have major repercussions on indirect climate forcing. Cloud droplet concentrations depend (nonlinearly) on concentrations of both anthropogenic and natural CCN. If many of the marine CCN are organic and natural, then because of the nonlinearity of CCN-droplet relationship, the sensitivity of drop concentrations to the addition of anthropogenic sulfate aerosols will be much lower than expected if organic aerosols are neglected.

Influence of Sample Composition on Aerosol Organic and Black Carbon Determinations

T. Novakov and C.E. Corrigan

Determining mass concentrations of major chemical species of biomass aerosols is a prerequisite for assessing the effects of biomass burning on the composition of the atmosphere and its influence on global and regional climate change. Accurate methods for chemical analyses of inorganic species are extensively used in most aerosol characterization studies. In contrast, techniques for characterizing carbonaceous material are much less accurate, and the results obtained by these methods are in many instances highly uncertain. Reasons for this situation are the chemical and physical complexity of carbonaceous (and other) aerosol material, sampling artifacts, and lack of appropriate standard materials.

We present results on characterization of filter-collected redwood (*Sequoia sempevirens*)-needle and eucalyptus smoke particles by thermal, optical, and solvent extraction methods. Our results demonstrate that organic and black carbon concentrations determined by thermal and optical methods are not only method dependent but also are critically influenced by the overall chemical composition of the samples. These conclusions are supported by the following: (1) The organic fraction of biomass smoke particles analyzed includes a component (ranging in concentration from about 6–20% of total carbon or from 16–30% of organic carbon) that is relatively nonvolatile and has a combustion temperature close to that of black carbon. (2) The presence of K or Na in biomass smoke samples lowers the combustion temperatures of this organic component and of black carbon, making their combustion properties indistinguishable. (3) About 20% of total organic material is nonvolatile when heated to 550°C in an inert atmosphere. Consequently, thermal methods that rely on a specific temperature to separate organic from black carbon may either underestimate or overestimate the black and organic carbon concentrations, depending on the amounts of Na and K and on the composition and concentration of organic material present in a sample. These analytical uncertainties and, under some conditions, absorption by organic material may contribute to the variability of empirically derived proportionality between light transmission through filter deposits and black carbon concentrations.

Organic Aerosols as Cloud Condensation Nuclei: A Laboratory Study of Cellulose Smoke Particles

T. Novakov, C.E. Corrigan, and C.A. Rivera-Carpio

Natural and anthropogenic water-soluble inorganic aerosol species (such as sulfate salts, sulfuric acid, and seasalt) are efficient cloud condensation nuclei (CCN), on which cloud droplets form by condensation of water vapor. Several studies have shown that biomass smoke particles, although composed mostly of organic material, are efficient CCN. However, because smoke particles (and atmospheric aerosol particles in general) consist of mixtures of organic and inorganic species, it has not been established whether the organic component is intrinsically CCN active, or whether the organic particles are intrinsically inactive and rendered CCN active only through association with water-soluble inorganic species. Results of our laboratory experiments demonstrate that biomass smoke particles, even when virtually free of inorganic water-soluble impurities, are intrinsically CCN active.

Our experiments were designed to establish whether the organic component itself can account for the CCN activity of biomass smoke particles. Answering this question is complicated by the fact that combustion of natural biomass inevitably results in particles that contain both the organic material and inorganic water-soluble species derived directly from the fuels. Our approach was to perform experiments with smoke particles practically free of inorganic impurities generated by combustion of pure cellulose, a surrogate biomass fuel.

Our experiments consisted of determining CCN number concentrations at 0.5% and 0.3% supersaturation, total particle number concentrations (or condensation nuclei, CN), and particle number size distributions of smoke particles produced by the smoldering combustion of purified cellulose (ash content ≈ 0.008%). We chose smoldering burning because it produces much higher yields of organic particulate matter than does flaming combustion, and it makes maintaining a reasonably steady smoke output easier. Smoke particles were analyzed for major water-soluble inorganic ions by ion chromatography and for carbonaceous material by Evolved Gas Analysis (EGA). Smoke samples were analyzed by EGA before and after water extraction. The results of chemical analyses show that the cellulose smoke is virtually free of inorganic water-soluble species and composed of completely water-soluble organic material.

The fraction of cellulose smoke particles acting as CCN at 0.5% and 0.3% supersaturation (i.e. the CCN/CN ratio) was determined by simultaneously measuring the CN and CCN number concentrations in a dilution chamber. These measurements resulted in an average CCN/CN ratio of 0.97 ± 0.15. The fact that the CCN/CN ratios are close to unity clearly demonstrates that these smoke particles are efficient CCN at the two supersaturations measured.

Our results demonstrate that organic particles essentially free of inorganic constituents, generated by smoldering combustion of cellulose, are completely water soluble and CCN active. These results provide evidence that some classes of aerosol organic material may act as CCN independently of the water-soluble inorganic species.

Ecological Systems

Aquatic Toxicology

S. Anderson and J. Jelinski

The broad goal of our research is to elucidate chronic and sublethal effects of exposure to toxic substances on aquatic ecosystems. Our studies cover a diverse range of interests from problem-focused studies on San Francisco Bay to more basic efforts to evaluate the effects of genotoxic substances on fish and invertebrates. Selected aspects of our work on the Bay have been completed this year. These projects, which have been conducted in collaboration with Dr. John Knezovich of Lawrence Livermore National Laboratory, are described below.

Determinants of sediment toxicity in San Francisco Bay

We recently completed a review of factors contributing to sediment toxicity in San Francisco Bay. We assembled a large database of sediment toxicity and chemistry data and evaluated several topical questions. These included: (1) the potential effects of sediment grain size in contributing to artefactual responses in toxicity tests; (2) toxicity observed at reference stations in the Bay; (3) relationships between sediment chemistry and toxicity; and (4) new approaches to evaluating bioaccumulation. We further evaluated the utility of national sediment quality guidelines for application in San Francisco Bay. Among our key conclusions was a recommendation that region-specific sediment quality guidelines be developed, because use of national guidelines will not result in meaningful improvements in sediment quality. Our research is being used by regulatory agencies to develop new approaches to sediment quality management.

Evaluation of sulfide tolerances of four marine toxicity test species

Toxicity tests using selected model animals are used to assess the effects of contaminants on sediment-dwelling organisms. Frequently, results of these tests are used to determine suitable disposal options for dredged sediments that may be contaminated with toxic substances. Recently, there has been widespread concern that sulfides, naturally-occurring in sediments, may result in artefactual toxicity in sediment toxicity tests. Despite widespread national concern, tolerances of the principle toxicity test species had never before been evaluated. We investigated the sulfide tolerances of four marine species that are commonly used to evaluate amphipod survival in bulk sediment (*Rhepoxynius abronius* and *Eohaustorius estuarius*) and embryo development in pore water (*Mytilus edulis* and *Strongylocentrotus purpuratus*). Because sulfide is volatile and subject to oxidation under static exposure conditions, we used sealed static and flow-through exposure systems to control the concentrations of sulfide to which organisms were exposed. Because the sensitivities of these organisms to sulfide have not been reported previously, this study provides benchmark data for evaluating the potential contribution of sulfides as a confounding factor in sediment and pore-water toxicity tests. These data have recently been used by the United States Environmental Protection Agency regional office in San Francisco to provide new guidance on sulfide toxicity to applicants for dredged materials disposal permits.

Developing regional sediment quality guidelines for metals in San Francisco Bay

Development of site-specific sediment quality guidelines is an important consideration for San Francisco Bay. These would be used to establish accurate cleanup targets at hazardous waste sites and would also be used to guide appropriate disposal options for dredged sediments. For metals, the development of such guidelines must include both chemical analyses that consider the partitioning of metals as well as toxicity tests that evaluate the effect-thresholds for metals. The study below describes techniques for evaluating metals partitioning as well as for testing toxicity using pore-water exposures.

Application of pore-water toxicity testing to development of site-specific sediment quality objectives for metals was explored in our study. We used metal-spiked pore-water bioassays to investigate the general utility of pore-water test techniques, and we evaluated variability in pore-water toxicity at a reference site in San Francisco Bay. Additionally, we developed a baseline of acid volatile sulfide (AVS) and sequentially extracted metals (SEM) data for San Francisco Bay that are useful in formulating a tiered approach to site-specific objective development. Metals concentrations eliciting toxic responses in pore water versus seawater varied less than a factor of 2.5 for a range of species and metals, with the exception of cadmium-exposed amphipods for which effect-levels in pore water were 5.14 to 4.63 times higher than those observed for seawater. Spiked pore-water bioassays were generally feasible, including an amphipod test conducted in 50 ml of pore water rather than in solid phase sediments. Nevertheless, operational parameters for conducting the tests must be carefully defined. In the reference site survey, pore-water toxicity varied little within a defined geographic region. Variation in SEM/AVS was moderate throughout the Bay. SEM values varied by less than a factor of 3. The lowest measured mean AVS value was 0.73 and the highest was 39.6. SEM/AVS ratios indicated that metals were not contributing to toxicity at any of the sites we studied in the Bay. In contrast, toxicity possibly attributable to ammonia and sulfides was observable at disparate sites. We concluded that site-specific objectives for metals should be developed using a tiered approach that includes both toxicity assessment and determination of SEM/AVS. Many aspects of actual implementation of such an approach, including field replicate variation, require further research.

References

Anderson SL, Knezovich JP, Jelinski J, Steichen DJ. *The Utility of Using Pore-Water Toxicity Testing to Develop Site-Specific Marine Sediment Quality Objectives for Metals.* Lawrence Berkeley National Laboratory Report No. LBL-37165, 1995. (also submitted to *Marine Environmental Research*)

Knezovich JP, Steichen DJ, Jelinski J, Anderson SL. Sulfide Tolerances of Four Marine Species Used to Evaluate Sediment and Pore-Water Toxicity. Lawrence Livermore National Laboratory Report No. UCRL-JC-121893 (1995). (*Bull. Environ. Contam. Toxicol.*, in press)

Hoffman ER, Anderson SL, Knezovich JP. *Determinants of Sediment Toxicity in San Francisco Bay: Final Report—December 1994.* Lawrence Berkeley National Laboratory No. LBL-36592 (1994).

Human Health Risk Assessment Of Environmental Pollutants

R. Goth-Goldstein

The goal of this research is to develop relevant cell systems that can help evaluate the health risk of environmental pollutants to humans. Presently, human health risk assessment is primarily based on data obtained from animal experiments. However, a number of uncertainties are inherent to animal experiments. First, the extrapolation from the very high doses typically used in animal experiments to the low doses to which humans are usually exposed is problematic. Secondly, there are marked species differences in the metabolic activation of toxins, leading to a different spectrum of DNA adducts. Finally, humans and rodents (the animals most commonly used for risk assessment studies) show major differences in the repair of these DNA adducts. Studies using human cell systems should be used to complement animal experiments, since results obtained from human cells can be considered relevant to humans. In the future, human cell systems might even substitute the expensive and unpopular use of animals as a screening tool for risk assessment.

Many chemicals are not harmful to health unless they are metabolized to an active form. Activation actually represents the first step of detoxification and elimination of a xenobiotic. In the body, metabolic activation occurs in certain tissues, the major site of metabolism being the liver, but other tissues also can activate foreign chemicals to a lesser extent. Cells most efficient in metabolic activation are of the epithelial type. Epithelial cells are defined by their origin during embryonic development. Fibroblasts represent another cell type. Even though fibroblasts are generally easier to grow in cell culture, they have a very low capacity to metabolize environmental pollutants. Therefore, epithelial cells competent in metabolic activation of environmental toxins are more useful for evaluating the toxicity of xenobiotics. In addition, since more than 80% of all human tumors arise in tissues of epithelial origin, assays using this type of cells would be most relevant for assessing the carcinogenic potency of chemicals.

Polycyclic aromatic hydrocarbons (PAHs) like benzo(a)pyrene are found in substantial amounts in the environment, and it is widely recognized that many of them have toxic, genotoxic, or carcinogenic effects. My laboratory has developed a bioassay using human epithelial cells to evaluate the presence of PAHs in complex mixtures. We grow normal human mammary epithelial cells obtained from reduction mammoplasties. These cells are capable of metabolically activating PAHs; we can show that they express *CYP1A1*, the gene coding for cytochrome P4501A1, the major enzyme involved in PAH activation. *CYP1A1* expression can be increased by the presence of PAHs resulting in their faster metabolic activation. Our assay measures, under standardized conditions, the metabolism of ^{3}H-benzo(a) pyrene (BaP) by mammary cells after preincubation with an extract of the test sample. The presence of PAHs in the sample is indicated if cells, after being incubated with the sample, show increased metabolism of BaP compared to control cells. We developed this assay as part of an EPRI-initiated study to evaluate the health hazard of manufactured gas plant residues. These residues are coal tars, which consist of complex mixtures of compounds, especially aromatic hydrocarbons. Individual coal tars vary in their exact composition depending on the origin of the coal, the manufacturing process, and the method of disposal. But in all coal tars examined with our assay, two- and three-ring compounds are the major aromatic hydrocarbon components of the mixture, whereas four- and five-ring compounds account only for a few percent of the coal tar. The potency of coal tars from various sites was compared by measuring the induction of BaP metabolism after exposing cells to organic extracts of coal tar samples prepared by Soxhlet extraction. The potency of individual coal tar extracts varied not more than three-fold. We also compared coal tars and pure BaP in respect to their efficiency in inducing BaP metabolism; we found that coal tars were almost as potent as BaP itself, even though BaP represents less than 1% of the coal tar. This suggests that: (a) the main constituents of the coal tar, two- and three-ring compounds, also induce BaP-metabolism; (b) the interaction between individual PAHs potentiates their inducing effect; and (c) PAHs other than BaP are much stronger inducers of *CYP1A1*. We recently studied hypothesis (a) by examining a number of low-molecular-weight aromatic hydrocarbons in our assay. We found that one- to three-ring aromatic hydrocarbons do not induce BaP metabolism. Therefore, the strong inducing effect observed with coal tar extracts is either due to potentiating effects of constituents of the complex mixture or to other not yet identified PAHs.

Even though our assay represents only an indirect measure of genotoxicity, it was in overall agreement with other short-term assays (*e.g.*, DNA adducts, *CYP1A1* induction in mouse liver) and correlated with the outcome, cancer in the juvenile mouse.

Reference

Goth-Goldstein, R. "Molecular Biology and Health Research." Presentation given at 1995 EPRI EMF Science Seminar *Understanding and Integrating the Science*. March 20-22, 1995, Santa Clara, CA.

Predicting Optical Properties of Marine Aerosols

M.S. Quinby-Hunt, L.L. Erskine, and A.J. Hunt

This project studies the scattering properties of aerosols in the marine boundary layer (MBL; approximately 500 m above the sea surface) and their effect on visibility, light propagation, radiant transfer, and global albedo. Polarized light scattering due to the various components of aerosols is modeled to establish the merits of using polarized light scattering strategies to enhance visibility and image discrimination in the MBL. This project investigates which polarization parameters are the most useful to characterize the dominant components of MBL aerosols.

Polarization of light plays an important role in visibility and image discrimination in the MBL. Particles in the MBL affect visibility, cloud formation, radiative transfer, and the heating and cooling of the earth. Dense MBL hazes modify propagation of sunlight affecting both the intensity and polarization of light reaching the sea surface. Polarization information must be included for accurate radiant transfer calculations at the surface of and within the ocean. Sources of image degradation in the MBL include ambient light scattered by aerosols or reflected from the sea surface into the object-receiver path; near-forward scattering from the object into the detector, altering the point-spread function; and thermally-induced changes in the refractive index of air (effects of convection). Aerosols in the MBL affect visibility because they scatter or blur light from the object and/or they scatter ambient light into the object/detector path to reduce the contrast between the viewed scene and the background. Angle-dependent polarization of scattered light varies significantly with the size, shape, and real and imaginary components of the refractive indices of the particles. If the sun or other source of light is behind the object, near-forward scattered source light, dominated by large aerosol particles, significantly reduces contrast of naturally-lit scenes. If the source of illumination (e.g., the sun) is near or behind the detector, light backscattered by small particles into the detector is important in reducing contrast. Thus, depending on the circumstances, light scattering from any angle can interfere with visibility by introducing scattered light into the source detector path. Polarization may also affect observations made against an ocean backdrop as the state of polarization of light reflected and scattered by the sea varies. Glare may be highly polarized with the polarization varying considerably with sun position and sky conditions. Therefore, aerosols and sea conditions can dramatically influence visibility or image quality.

The angular dependence of the linear and circular polarization of light scattered in the MBL provides the most complete information regarding the aerosol characteristics obtainable by remote sensing. Measurements of the polarization properties of aerosols can be used to infer effective size distributions and refractive indices of aerosols without the problems of collection devices. The limited research on the scattering properties of atmospheric aerosols has been primarily with terrestrial aerosols. Few studies have investigated the polarization properties of scattered light in marine aerosols and even fewer using the fullest description of the polarization as embodied by the Mueller scattering matrix formalism.

Polarized scattering measurements have been made of water and sea water aerosols and aerosols of aqueous NaCl and $(NH_4)_2SO_4$ to simulate the sea-salt-containing (SSC) component of MBL aerosols under a variety of conditions. This component is important to visibility considerations as it the major contributor to the coarse fraction of the MBL aerosol and thus can result in significant forward scattering (i.e. scattering angles < 60°). Coarse fraction MBL aerosols also can alter visibility in the backscatter region (> 90°). The effect of varying humidity on the aerosols was examined. From the Mueller matrices of each aerosol, size distributions and relative complex refractive indices of the aerosol particles were determined. Mie scattering models were used to calculate the Mueller matrices for light scattered from combinations of Junge, Gaussian, and skewed distributions of spheres and coated spheres, of varying composition and refractive index.

Results

As predicted by our previous work (Quinby-Hunt MS, Hull PG, and Hunt AJ, "Predicting Polarization Properties of Marine Aerosols," presentation given at Ocean Optics XII, June 13-15, 1994, Bergen, Norway; published in *Proceedings of the SPIE, Ocean Optics XII, 2258*, 735-746), the polarization properties of light scattered by the SSC component of aerosols in the MBL were varied with size, refractive index, and size distribution of particles. These differences are instrumentally detectable. As the temperature in the desiccation system was increased, water was removed from the aerosol droplets, simulating a decrease in humidity. For all three solutions—seawater, NaCl, and $(NH_4)_2SO_4$—the aerosols deviate from sphericity at higher temperatures. NaCl shows the most pronounced deviation; $(NH_4)_2SO_4$ shows somewhat less. Seawater aerosols remain nearly spherical to higher temperatures.

Experiments and calculations confirmed that the use of polarization sensing techniques can reduce scattered light components and therefore improve visibility in the MBL. The optimum orientation of the polarizer and its efficacy in improving image contrast depend on both atmospheric conditions and the solar (illumination source)-viewer-target angle. Under conditions of high relative humidity, the polarized scattering from the SSC component of the MBL is well-described by rigorous calculations. As the humidity decreases the polarization signature from this component becomes more complex and is not readily described using Mie calculations. As MBL aerosols are highly complex and variable, and have profound effects on visibility, it would be prudent to design an agile polarization-sensing device to optimize strategies for improving visibility and image discrimination under a variety of conditions. The calculations and experimental work indicate that Mie calculations can produce reliable inputs for calculating radiant transfer under most atmospheric conditions; only very dry air masses need be excepted.

References

Erskine LL, Quinby-Hunt MS. *Polarization Properties of the Sea-Salt-Containing Component of Marine Aerosols.* Report to the Summer Undergraduate Research Program, California Institute of Technology, Pasadena, California (1995).

Quinby-Hunt MS, and Hunt AJ. "Role of Polarization in Light Propagation through the Marine Boundary Layer." Presented at the National Meeting, Optical Society of America, Special Session on Scattering and Absorption in the Ocean, Portland, Oregon, September 10-15, 1995.

The Oxidant and Antioxidant Balance in Wounds

J.J. Maguire, L. Packer, H. Kobuchi, T. Ogino, C. Wicke, and L. Marcocci

Immunity to infection is a complex cellular response that aids in maintaining protection from invading microorganisms. Our research focuses on the role of oxidants and antioxidants in the immune defense systems of white blood cells (leukocytes). The leukocyte's response to bacterial assault involves production of copious quantities of reactive oxidants and free radicals. This includes superoxide (O_2^-), hydrogen peroxide, sodium hypochlorite, hydroxyl radical (OH◊) and nitric oxide (NO). While these compounds can aid in the killing of invading bacteria, they can also damage the host. A balance exists between production and containment of these reactive compounds. The goal of this research is to understand this dynamic process.

Two types of leukocytes are used for these studies: neutrophils, which are the primary "front-line" leukocytes, and macrophages, which are more involved in chronic infections. Environmental pollutants, especially compounds that result in the biological formation of free radicals, can suppress the immune response and alter immunity adversely. These basic research projects are designed to better understand the functioning of leukocytes in order to devise ways to enhance immunity and decrease infectious diseases, especially in wounds.

Artificial Enhancement of the Respiratory Burst Activity *In Vitro*

Dehydroascorbate can enhance the rate of the respiratory burst at relatively low (10-50 μM) concentrations. A comprehensive study was undertaken of both the rat and human neutrophil respiratory burst activity in the presence of dehydroascorbate, measuring both the rate and the extent of the respiratory burst. Additions of dehydroascorbate can increase the respiratory burst rate and extent up to 25%.

In conditions where the respiratory burst activity is compromised (*e.g.*, in conditions of low oxygen tension or in suppressed temperature), an enhanced respiratory burst (both longer duration and rate) can enhance bactericidal activity. Preliminary studies have measured the respiratory burst of low pH and low oxygen tension. The respiratory burst is quite stable at pHs between 6.8-7.5, and the respiratory burst exhibits a high Km for oxygen. Subsequent measurements of the temperature dependence of the NADPH-oxygenase demonstrate very little sensitivity to temperature of the respiratory burst from 37 to 30°C. This indicates that the NADPH-oxygenase can function well in peripheral tissues where the temperature is frequently below core body temperature.

A surprising result was obtained upon heating isolated neutrophils. Temperatures of 40°C for 15 minutes (*in vitro*) can substantially impair the respiratory burst rate and extent. A heat shock of 42°C for just a few minutes will essentially destroy the NADPH-oxygenase. Human core temperatures are often at 40°C for long periods, so we are interested to determine if neutrophil NADPH-oxygenase is impaired in whole blood. Human whole blood (freshly drawn) was heated for 20 minutes and a control sample was heated for the same time at 37°C. Significant (20%) decreases in the NADPH-oxygenase were noted in the samples that were heated to 40°C. These results pose two questions: does fever in humans cause a suppression of the NADPH-oxygenase, and does this alter immunity? Enhancement of the neutrophil NADPH-oxygenase activity *in vitro* may have important clinical significance if NADPH-oxygenase enhancement can be shown to increase immunity.

Assessment of the Oxidant Capacity of Neutrophils

Studies in progress have shown that we can readily measure the ascorbate and vitamin E in isolated neutrophils. We have measured a significant decrease in the vitamin E content during incubation *in vitro* but there does not appear to be a decrease in the ascorbate content following NADPH-oxygenase activation. Future plans as outlined below include measurement of neutrophil glutathione, superoxide dismutase and catalase. As neutrophil bactericidal activity substantially involves the production of reactive radicals, the protective mechanisms of the neutrophil are very important for the protection of neutrophils from their own radical production.

Assessment of Oxidative Damage to Neutrophils

New studies have been undertaken to measure neutrophil nitro-tyrosine production. Nitric oxide production in rat neutrophils has been previously measured and reaction of *NO with* superoxide from the respiratory burst results in formation of peroxynitrite. Nitration of tyrosine residues of neutrophils provide an assessment of protein oxidative damage. The exact role of protein nitration is not clear as it may be involved in cell signaling, and certainly can alter the antigenicity of the cell surface. Preliminary measurements have shown that there is a time dependent formation of nitro-tyrosine, that it is increased by superoxide dismutase, and that the mechanism of its production is not known at this time. It is possible that nitration of tyrosines may prove useful in assessing actual cellular damage from chronic inflammation. The antioxidant capacity of neutrophils from both rats and humans in both the resting state as well as the activated state. Vitamin E, ascorbate, glutathione (reduced and oxidized), and the enzymes catalase and superoxide dismutase have been measured, and they certainly have a role in protecting the neutrophil from its own oxidants.

In vitro enhancement of the respiratory burst activity by antioxidant will continue to be measured. A water soluble derivative of vitamin E lacking the hydrophobic "tail," 2,2,5,7,8-penta-methyl-6-hydroxychromane (PMC), has been shown to readily exchange across cell membranes when added as an external antioxidant. This, in combination with the water soluble dehydroascorbate supplementation, may provide useful information on possible animal and human supplements to enhance the NADPH-oxygenase activity to improve immunity from infection.

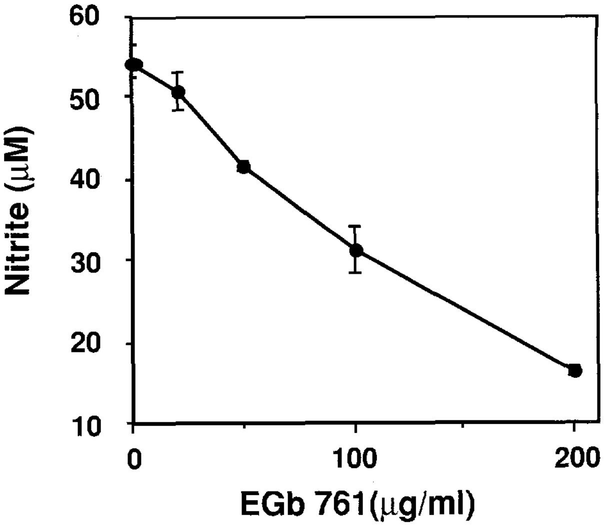

Figure 1. *Effect of EGb 761 on NO production by macrophages. RAW 264.7 macrophages (5 ×10^6 cells/ml/well) were stimulated with LPS plus IFN-g in the presence of various doses of EGb 761. After incubation for 20 h, nitrite in the conditioned medium was measured.*

Gingko Biloba extract (EGb 761) Suppresses Nitric oxide Production in Macrophages

Reactive oxygen species (ROS) generated by a partial reduction of O_2, pose a serious threat to tissue and vital organs and cells. It is thought that ROS have been implicated in the pathogenesis of inflammation, cancer and atherosclerosis. Therefore, antioxidants, including natural compounds that can scavenge ROS or prevent their formation, could be therapeutic value. From this perspective, we have studied the antioxidant ability of Gingko biloba extract (EGb 761), which is a natural antioxidant.

EGb 761 is a defined extract prepared from the leaves of Ginkgo biloba that has been effective in the treatment of disorders related to oxidative stress. A large amount of NO produced by macrophages is implicated in several pathophysiological processes including immune-mediated cytotoxicity and cell killing. The present study was designed to gain insight of EGb 761 on NO production in murine macrophage cell line RAW 264.7.

Induction of nitric oxide synthase (iNOS) is known to be inhibited by various reagents, such as cytokines and steroid hormones, which can affect transcriptional or post-transcriptional regulation. EGb 761 has been found to be a new inhibitor of NO production. EGb 761 inhibited NO production from mouse macrophages activated with lipopolysaccharides (LPS) and gamma interferon (IFN-g) in a dose dependent manner (Fig. 1). The inhibition of NO production by EGb 761 at the highest dose was not due to cell death.

EGb 761 also inhibited the expression of iNOS mRNA in macrophages acti-

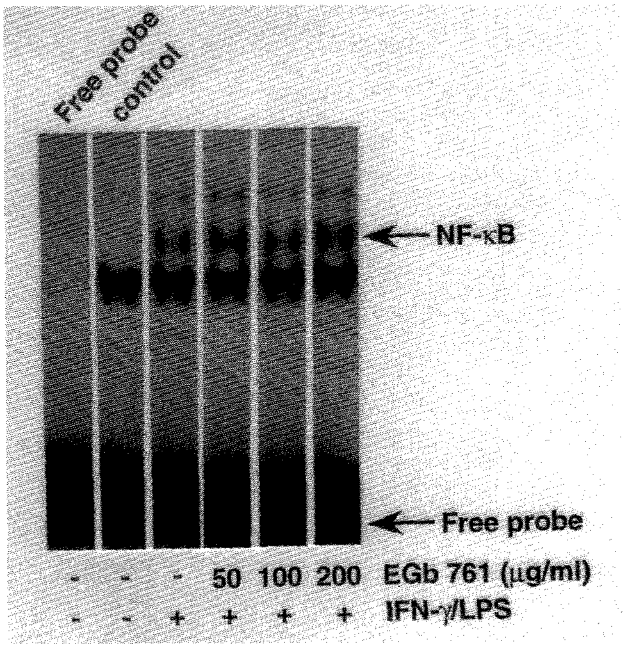

Figure 2. *Effect of EGb 761 on the expression of iNOS mRNA in macrophages. Macrophages were treated with various doses of EGb 761 and treatment time as indicated, and stimulated with LPS plus IFN-g. After incubation for 7 h, cells were harvested, and total RNA was applied to RT-PCR*

vated with LPS and IFN-g (Fig. 2). This result suggested that inhibitory effects on NO production in macrophages occurs by interference with expression of iNOS of EGb 761. However, the amount of suppression was relatively small as compared with the amount of inhibition of NO production. Consequently, the scavenging effect of EGb 761 against NO itself, which we have previously demonstrated, might in part also be responsible for its inhibitory effect.

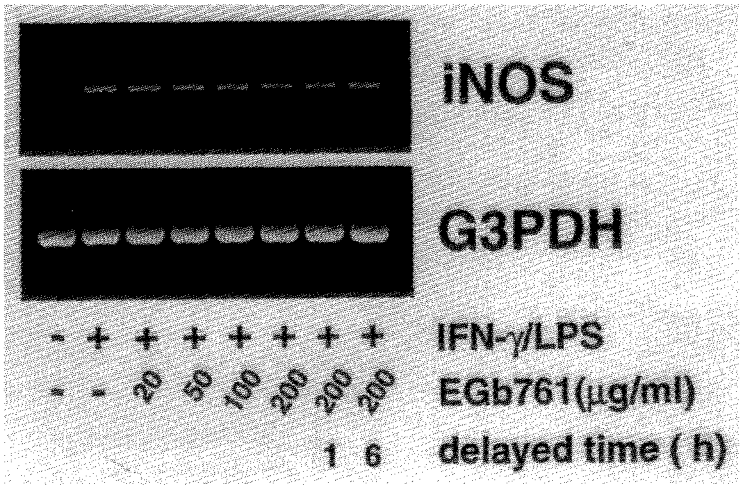

Figure 4. *Effect of EGb 761 or flavonoids against activity of rat brain protein kinase C. PKC inhibitory effect of EGb 761 or flavonoids was assessed by measuring the incorporation of ^{32}P from [g-^{32}P] ATP into PKC substrate.*

NF-kB (a "trigger" protein that is especially sensitive to cellular oxidant stress) activation is an essential factor in iNOS expression. To assess the effect of EGb 761 on early stages of iNOS gene expression, activation of the NF-kB in macrophages was examined using electrophoretic mobility shift assay. EGb 761 treatment along with LPS and IFN-g did not affect the activation of NF-kB, even at the highest dose (200 μg/ml) which had been shown to markedly inhibit the expression of iNOS mRNA (Fig. 3, next page). These results indicate that EGb 761 may also be acting at another site, including post-transcriptional modulation (e.g., stabilizing of mRNA) or direct inhibition of iNOS enzyme activity.

Protein kinase C (PKC) plays an important role in a signal transduction in various cells. Moreover, it is thought that PKC may be involved in the induction of NOS. To obtain further insight into the mechanisms of EGb 761, we examined the effect of EGb 761 using PKC partially purified from rat brain. EGb 761 inhibited activity of rat brain PKC in a dose dependent manner (Fig. 4). Moreover, quercetin, a prominent ingredient of EGb 761, also inhibited the activity of PKC. However, while rutin (another antioxidant ingredient) inhibited the activity of PKC, the inhibitory action was weak. These results suggested that NO inhibitory action of EGb 761 in macrophages was implicated in the inhibition of PKC activity.

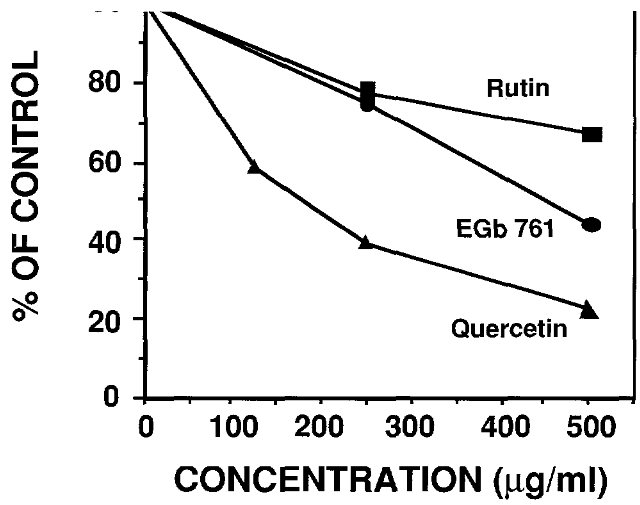

Figure 3. *Effect of EGb 761 on the DNA binding activity of NF-kB in activated macrophages. Macrophages were treated with the indicated dose of EGb 761 and stimulated with LPS plus IFN-g. After 1 h incubation, nuclear extracts were isolated and EMSAs were performed.*

The present study demonstrated that the inhibitory mechanism of EGb 761 on NO production in macrophages may be due to inhibition of iNOS mRNA expression. Quercetin, one of the flavonoid components of EGb 761, may be involved in this inhibition. Moreover, it was considered that a plausible mechanism for suppression of NO production by EGb 761 could be because of the inhibition of protein kinase C in macrophages by these flavonoid compounds.

References

Marcocci L, Maguire JJ, Packer L. Nitecapone—A nitric oxide radical scavenger. *Biochemistry and Molecular Biology International* 1994;34: 531.

Marcocci L, Maguire JJ, Droy-Lefaix MT, Packer L. The nitric oxide-scavenging properties of Ginkgo Biloba Extract EGb 761. *Biochemical And Biophysical Research Communications* 1994; 201: 748.

Environmental Contaminants: Toxicology and Bioremediation

R.J. Mehlhorn, S. Chen, G. Ishkhanova, S. Jovanovich, and K. Moore

Environmental contaminants comprise a diversity of chemicals ranging from highly toxic gases that occasionally escape from industrial processes to nuisance pollutants posing relatively few health or ecosystem threats but deemed to be aesthetically offensive, e.g., certain colorants in waste water. Airborne toxins and carcinogens, such as those in tobacco smoke, are particularly hazardous to humans because they can reach body tissues without passing through the liver, which detoxifies most contaminants in food and water. Research on the adverse health effects of tobacco smoke has sought to understand toxicity mechanisms and to quantify risk associated with both mainstream and second-hand tobacco smoke. While considerable progress has been made on acute molecular damage mechanisms of tobacco smoke toxins like nicotine, cyanide and carbon monoxide, and on some chronic damage mechanisms, *e.g.*, reactions of tobacco-specific carcinogens with DNA, many aspects of tobacco toxicity remain to be elucidated. One important unresolved question concerns the possible activation of molecules in tobacco smoke to more toxic products after they have dissolved in body fluids. Our project is investigating one facet of this question by studying chemical and biochemical transformations of tobacco smoke in human blood.

Our other major project is concerned with water pollutants produced in textile dyeing. Current industrial practice leads to the discharge of considerable volumes of dye-colored water and auxiliary chemicals into waste-streams, posing environmental concerns and economic loss. Our project seeks to recover the dyes, thus improving dye utilization and preventing water contamination. Dye recovery is achieved with biological agents, including microbial biomass and chemically modified biopolymers. We have demonstrated the feasibility of selectively removing and recovering colorants from dye bath waters, producing waters containing a variety of chemical additives that can be fed back into the process stream for new dyeing applications.

We seek an improved understanding of tobacco-smoke toxicity mechanisms and the development of new technology, utilizing biomass-derived sorbents, for removing and recovering textile dyes and other valuable chemicals from water.

Our principal experimental approach is electron spin resonance (ESR), a highly specific method that detects the magnetic moments of reactive free radicals, transition metal ions and "spin-labeled" organic molecules. This method has been used to analyze biological structures with the goal of optimizing the utilization of biomass for resource recovery. ESR has also been used to develop novel markers of tobacco smoke damage, which are being applied to the analysis of tobacco-smoke toxicity mechanisms.

Research Highlights

Cigarette smoke-induced damage in human blood As reported previously, we have demonstrated that glutathione is depleted when human blood is exposed to gas-phase cigarette smoke. Our subsequent efforts have focused on developing tools for understanding not only the mechanisms of such low molecular weight antioxidant depletion but also for elucidating reaction pathways that inhibit protective enzymes. A major thesis of this work is that cyanide, known to be present in tobacco smoke at relatively high concentrations, blocks vital enzymatic protective systems, leading to uncontrolled free radical reactions whose consequences include the formation of new carcinogenic agents. Our initial observation of an inactivation of ascorbic acid oxidase in cigarette smoke-treated blood demonstrated a potent inhibitory effect of smoke-borne cyanide on the activity of a copper enzyme. More recently, we found evidence of free radical formation in cyanide-treated blood with spin-trapping studies utilizing Na^{13}CN. Treatment of human blood with 20 mM cyanide in the presence of the spin trap DMPO (5,5-dimethyl-1-pyroline N-oxide) elicited an ESR signal of the cyanidyl radical, demonstrating that otherwise unstressed intact red blood cells generate free radicals in the presence of cyanide. We had long been aware that cyanide inhibition of superoxide dismutase and catalase would compromise overall antioxidant protection in the erythrocyte, but learned only recently of the potential inhibition of the seleno-enzyme glutathione peroxidase under the conditions of our experiments. Thus it appears that all of the major peroxide-scavenging systems may be compromised by cyanide, leaving the cell unprotected from the destructive effects of highly reactive peroxide-derived oxyradicals. Currently, we are analyzing the extent and duration of the tobacco smoke-induced inhibition of glutathione peroxidase and other antioxidant enzymes.

To investigate the possible formation of new carcinogens when tobacco smoke reacts with blood, we have synthesized new ESR probes to detect nitrosation of amino groups. The principle being exploited is the conversion of highly soluble secondary amines to poorly water-soluble nitrosamines. Model system studies have demonstrated that our probes undergo major partitioning changes in blood upon nitrosation, seen as a conversion of an aqueous ESR signal to a membrane- and albumin-bound ESR signal as the secondary amine is converted to its nitrosamine derivative. A control tertiary amine probe was unaffected by nitrosation, as expected, and serves to assess the effects of alternative tobacco smoke reactions, e.g., alterations of membrane structure by hydrophobic molecules in gas-phase smoke.

Dye recovery from textile waste waters. Several effective biosorbents have been developed for use in both continuous and batch-mode dyeing operations. Chemical modification of some biosorbents has yielded materials suitable for repeated use under harsh conditions prevalent in the industry. Economics of biomass production have been improved with the introduction of alternative biosorbents. Some biosorbent materials we have developed are suitable for direct use with existing machinery, thus avoiding costs associated with the engineering and construction of new equipment. The original dye recovery scheme, based on reversible biosorption, has been expanded. As our understanding of dye-biomass interactions evolved, we discovered a variety of schemes to control the solubility of dyes in water and how to exploit this understanding to develop rapid filtration schemes that could augment biosorption. These efforts have led to the development of the concept of a multiphase dye recovery system comprising both filtration and sorption to achieve separation of dyes from process waters, followed by the recovery of concentrated colorants for reuse. The processed waters, containing valuable chemical adjuncts for efficient dyeing, are suitable for recycling, allowing for a near zero-discharge dyeing operations.

Sponsors

Support from the following sources was provided through the U.S. Department of Energy under Contract No. DE-AC03-76SF00098:

- Director, Office of Energy Research, U.S. Department of Energy:
  - Office of Basic Energy Sciences, Chemical Sciences Division
  - Office of Health and Environmental Research, Environmental Sciences Division

- Pittsburgh Energy Technology Center
- Battelle Pacific Northwest Laboratory
- National Aeronautics and Space Administration, Microgravity Science and Applications Division
- Oak Ridge National Laboratory
- Office of Naval Research
- University of California, Tobacco-Related Disease Research Program, Grant RT0240
- U.S. Army Corp. of Engineers
- U.S. Department of Energy AMTEX program
- U.S. Environmental Protection Agency
- University of California/NIEHS
- University of California, San Francisco/NIH